

UNIVERSITY OF KWAZULU-NATAL

**ENHANCED SPECTRAL EFFICIENCY SCHEMES FOR
SPACE-TIME BLOCK CODED SPATIAL
MODULATION**

Sibusiso Thabiso Motsa

Supervised by:

Professor HongJun Xu

2019

ENHANCED SPECTRAL EFFICIENCY SCHEMES FOR SPACE- TIME BLOCK CODED SPATIAL MODULATION

Sibusiso Thabiso Motsa

Supervised by:

Professor HongJun Xu

School of Engineering, Electrical, Electronic and Computer Engineering, University of
KwaZulu-Natal, Durban, South Africa

Submitted in fulfilment of the degree of Master of Science in Engineering,

October 2019

As the candidate's supervisor I have approved the submission of this dissertation.

Signed: _____

Name: Professor HongJun Xu

Date:

DECLARATION-PLAGIARISIM

I, Sibusiso Thabiso Motsa, declare that

- i. The research reported in this dissertation, except where otherwise indicated, is my original work.
- ii. This dissertation has not been submitted for any degree or examination at any other university.
- iii. This dissertation does not contain other persons' data, pictures, graphs or other information, unless specifically acknowledged as being sourced from other persons.
- iv. This dissertation does not contain other persons' writing, unless specifically acknowledged as being sourced from other researchers. Where other written sources have been quoted, then:
 - a. Their words have been re-written, but the general information attributed to them has been referenced;
 - b. Where their exact words have been used, their writing has been placed inside quotation marks, and referenced.
- v. This dissertation does not contain text, graphics or tables copied and pasted from the Internet, unless specifically acknowledged, and the source being detailed in the dissertation and in the References sections.

Signed: _____

Acknowledgements

Firstly, I give thanks and praise to the Creator for the opportunity and strength during my academic journey and the gift of life.

I would like to thank my supervisor, Prof Xu, for his continued support, assistance and guidance on my research work and writing skills. Without your avid participation and input, the validity of this work would not have been successfully completed. I also like to thank you for the life lessons you imparted on me.

To my colleagues in the Faculty of Electrical, Electronic and Computer engineering, thank you for all the assistance you afforded to me.

Finally, I would like to express my profound gratitude to my parents, siblings and significant other, for their relentless support and encouragement throughout my years of study and research. This accomplishment would not have been without them. Thank you.

Abstract

The ever-growing demand for high data rate, low latency and energy efficient transmission schemes has seen an increasing popularity of multiple-input multiple-output (MIMO) scheme. One such scheme is the orthogonal space-time block code (STBC) scheme introduced by Alamouti which provides full diversity without sacrificing its data rate. Introduction of spatial multiplexing to STBC through spatial modulation (SM) improves the performance and spectral efficiency whilst eliminating transmit antenna synchronization and inter-channel interference (ICI) at the receiver. In this dissertation, we investigate and evaluate the error performance of both STBC and SM MIMO schemes. As such, we exploit the advantage of both schemes in space-time block coded spatial modulation (STBC-SM) scheme resulting in a high spectral efficient scheme.

Motivated by the requisite for higher data rate transmission schemes, we expand the orthogonal STBC transmission matrix to further improve the spectral efficiency of space-time block coded spatial modulation. The fundamental idea is keeping the size of the amplitude/phase modulator (APM) symbol set of STBC the same. Therefore, unitary matrix transformation technique is introduced to the conventional STBC matrix. This technique prevents an increase in the peak-to-average power ratio of the transmitted symbols. A decrease in the phase angle of the unitary matrix yields an increase in the number of information bits transmitted, subsequently increasing the spectral efficiency of a system.

A new system referred to as enhanced spectral efficiency space-time block coded spatial modulation (E-STBC-SM) is proposed. Moreover, a tight closed-form lower-bound is derived to estimate the average BER of the E-STBC-SM system over Rayleigh frequency-flat fading channel and validated with Monte Carlo simulations. Comparisons of the proposed E-STBC-SM scheme and conventional STBC-SM scheme are carried out with four receive antennas in all cases. The E-STBC-SM scheme virtually retains the BER performance of the STBC-SM scheme with a maximum attenuation of 0.6 dB throughout modulation order 16, 32 and 64 of a PSK modulator. An increase of between 2 to 5 information bits are obtained across the motioned modulation orders through altering of the phase angle of the unitary matrix transform incorporated with the conventional STBC-SM scheme thus improving the spectral efficiency. In a rare occurrence of $M = 32$ and $\theta = \frac{\pi}{2}$ configured E-STBC-SM scheme, an improvement of 0.2 dB in error performance was experienced.

Table of Contents

DECLARATION-PLAGIARISIM.....	ii
Acknowledgements.....	iii
Abstract.....	iv
Table of Contents.....	v
List of Figures.....	ix
List of Tables.....	xi
List of acronyms.....	xii
Chapter 1 An overview of wireless communications.....	1
1.1 Introduction.....	1
1.2 An overview of channel fading.....	4
1.2.1 Multipath Fading Channels.....	4
1.2.2 Rayleigh Fading Model.....	4
1.3 An Outline of Diversity Techniques.....	5
1.3.1 Time.....	5
1.3.2 Frequency.....	5
1.2.3 Space.....	5

1.2.4 Signal Space	5
1.4 An Overview of Spectral Efficiency Enhancement Techniques	6
1.3.1 Spectral Efficiency	6
1.3.2 Spectral Efficiency Enhancement Techniques	6
1.3.2.1 Alamouti Space-time Block Codes	7
1.3.2.2 Efficiency-Improved Alamouti Code	7
Notation	8
1.5 The conventional MIMO system.....	9
1.5.1 Space-Time Block Coded Spatial Modulation	11
1.5.2 Space-Time Block Coded Spatial Modulation with Labelling Diversity.....	11
1.5.3 Super-orthogonal Space-Time Block Code Using a Unitary Expansion	12
1.6 Motivation and Contributions	13
1.6.1 Proposed Enhanced Spectral efficiency of M-PSK STBC-SM using unitary matrices	13
1.7 Structure of the Dissertation.....	14
Chapter 2 Alamouti space-time block coding.....	15
2.1. Introduction	15
2.2. Space-time Block Coding.....	15
2.3. Transmission	16
2.4. Detection	18
2.5. BER Performance Analysis.....	19

2.6. Results	20
2.6.1. 16-PSK with MRC vs 16-PSK ALAMOUTI STBC	22
2.7. Chapter synopsis and Conclusions.....	25
Chapter 3 Spatial Modulation	26
3.1. Introduction	26
3.2 Transmission	26
3.3. Spatial Modulation Detection.....	30
3.4. Performance Analysis	31
3.5. Analytical and Simulation Results	32
3.6 Chapter Synopsis.....	36
Chapter 4 Space-Time Block Coded Spatial Modulation.....	37
4.1. Introduction	37
4.2. Transmission	37
4.3. Detection	39
4.4. Performance Analysis	40
4.5. Analytical and Simulation Results	42
4.6. Chapter Synopsis.....	46
Chapter 5 Enhanced Spectral Efficiency of Alamouti Space-time block coded Spatial Modulation Using Unitary Matrix Transformation (E-STBC-SM)	47

5.1. Introduction	47
5.2. The STBC Expansion.....	48
5.3. Transmission	50
5.4. Detection	52
5.5. Theoretical Analysis of E-STBC-SM	53
5.5.1. Analytical BER for Estimated Symbol Pair	53
5.5.2. Analytical BER for the Phase Symbol	54
5.6. Analytical and Simulation results	56
Chapter 6 Conclusion and future work	66
6.1. Conclusion.....	66
6.2. Future Work	70
6.2.1 Low complexity detection	70
6.2.2. Convolutional coding/ TCM.....	70
Appendix A.....	71
References.....	76

List of Figures

Figure 1-1: Demonstration of an $N_r \times N_t$ MIMO system	10
Figure 2-1: $N_r \times 2$ Alamouti STBC	17
Figure 2-2: M-PSK Alamouti STBC Analytical and Monte-Carlo simulations.....	21
Figure 2-3: M-QAM Alamouti STBC Analytical and Monte-Carlo simulations.....	22
Figure 2-4: Comparison of $2 \times N_r$ 16-PSK Alamouti STBC Vs 16-PSK SISO scheme.....	23
Figure 2-5: Comparison of 16-PSK Alamouti STBC Schemes with MRC and SISO schemes...	24
Figure 3-1: $N_r \times N_t$ SM System model.....	27
Figure 3-2: Monte Carlo simulation and Theoretical bounds for 16-PSK.....	33
Figure 3-3: Monte Carlo simulation and Theoretical bounds for 16-PSK and 8-PSK.....	34
Figure 3-4: Monte Carlo simulation and Theoretical bounds for 4-QAM and 16-QAM.....	35
Figure 4-1: Alamouti STBC-SM system model [6].....	38
Figure 4-2: Monte Carlo simulation and Theoretical bounds for 8-PSK STBC-SM and 16-PSK STBC-SM	43
Figure 4-3: Monte Carlo simulation and Theoretical bounds for 16-QAM STBC-SM and 64- QAM STBC-SM.....	44
Figure 4-4: BER performance of 8/16-PSK STBC-SM and 8/16-PSK SM.....	45
Figure 5-1: E-STBC-SM system model.....	50
Figure 5-2: Theoretical and Simulated Average BER	57
Figure 5-3: BER performance of 16-PSK STBC-SM and 16-PSK E-STBC-SM	58

Figure 5-4: BER performance of 32-PSK Alamouti STBC-SM and 32-PSK Alamouti E-STBC-SM.....	59
Figure 5-5: BER performance of 64-PSK Alamouti STBC-SM and 64-PSK Alamouti E-STBC-SM.....	60
Figure 5-6: BER performance of 64-QAM Alamouti STBC-SM and 64-QAM Alamouti E-STBC-SM	61
Figure 5-7: Comparing the Performance of systems with 12 bits per frame	63
Figure 5-8: Comparing the Performance of systems with 14 bits per frame	64

List of Tables

Table 3-1: Gray-coded constellation points for 8-PSK-SM modulation order.....	28
Table 5-1: Additional bits with corresponding rotational angles.....	49
Table 5-2: Summary of Throughput, Performance Attenuation, and Spectral Efficiency	62
Table 6-1: SNR gain (dB) of SM compared to STBC-SM at BER of 10^{-5}	67
Table 6-2: % Spectral Efficiency improvement of E-STBC-SM against STBC-SM.....	68
Table 6-3: % Attenuation of E-STBC-SM against STBC-SM.....	69

List of acronyms

ABEP	Average Bit Error Probability
APM	Amplitude/Phase Modulation
AWGN	Additive-White Gaussian Noise
BEP	Bit Error Probability
BER	Bit Error Rate
BPCU	Bit Per Channel Use
CSI	Channel State Information
HR	High Rate
IAS	Inter-Antenna Synchronization
ICI	Inter-Channel Interference
IOT	Internet of Things
i.i.d.	Independent and Identically Distributed
I-IOT	Industrial Internet of Things
LC	Low Complexity
LOS	Line-Of-Sight
MCS	Modulation and Coding Scheme
MGF	Moment Generation Function
MIMO	Multiple-Input Multiple-Output
MISO	Multiple-Input Single-Output
ML	Maximum-Likelihood
MRC	Maximum Ratio Combining
MPSK	M-ary Phase Shift Keying
MQAM	M-ary Quadrature Amplitude Modulation
MSB	Most Significant Bit
PAPR	Peak-to-Average Ratio
pcu	Per channel use
PDF	Probability Density Function
PEP	Pairwise Error Probability
PSK	Phase Shift Keying

QAM	Quadrature Amplitude Modulation
QPSK	Quadrature Phase Shift Keying
RV	Random Variable
SC	Selective Combining
SER	Symbol Error Ratio
SM	Spatial Modulation
SM-LD	Spatial Modulation Labelling Diversity
SNR	Signal-to-Noise Ratio
SISO	Single-Input Single-Output
STBC	Space-Time Block Coding
STBC-CSM	Space-Time Block Coded Spatial Modulation with Cyclic Structure
STBC-SM	Space-Time Block Coded Spatial Modulation
STTC	Space-Time Trellis Codes
SWC	Switched Combining
TAC	Transmit Antenna Combining
TCM	Trellis Coded Modulation
V-BLAST	Vertical Bell Labs Layered Space-Time Architecture

Chapter 1

An overview of wireless communications

1.1 Introduction

The field of wireless communication has been in the perpetual study since Marconi pioneered and effectively demonstrated the first use of radio transmission in 1895. However, the past two decades have experienced an exponentially growing demand for wireless transmission of speech, data, and video signals thereby necessitating an increase at the rate at which research and development of more efficient and reliable communication technologies are carried out [1]. By the year 2020, it is envisaged that an excess of 50 billion devices will be connected to the internet [2]. 5G, the next generation of wireless networks expected to be introduced in the 2020 timeframe, is characterized by blazing speeds, robustness of the network and ultra-low latencies that will permit massive amounts of data to be transmitted between connected devices, systems, and infrastructure in near real-time. As such, 5G will be the backbone of the Fourth Industrial Revolution (Industry 4.0) which has dawned upon the 21st century. In the context of the latter, the vision is the integration of massively installed network technologies and smart computing in manufacturing environment and industrial production for the purpose of automation, control, reliability, and involving the development of an Industrial Internet of Things (I-IoT) which is dedicated in adopting the IoT (Internet of Things) [3]. Principally, IoT is the inter-connection of massively deployed and distributed physical devices that can be used to monitor and control objects in cyber-Physical systems such as smart cities or smart grid leading to a smart and connected world where a large number of everyday devices are interconnected [4]. Reliable, robust and low latency wireless communication systems are critical characteristics in realizing the full potential envisaged for the Fourth industrial revolution.

Nonetheless, there remain practical constraints in wireless communication systems such as power consumption, computational complexity and costly hardware which form the primary factors to be considered in the designing of these systems. The channel between transmitter and receiver of a wireless communication system is susceptible to various kinds of attenuation that include path loss, noise, and multipath attenuation but to mention a few, that can, in turn, corrupt or/and distort the transmitted signal. The naturally occurring disturbance due to the fluctuation of electrical distribution and other physical factors known as noise is assumed to follow a Gaussian distribution. Moreover, the noise displays uniform power across the frequency band, hence it is said to be white. This noise is commonly referred to as Additive white Gaussian noise (AWGN) because it is superimposed to the signal at the receiver. A further look at these impediments narrowed down to the context of this dissertation are discussed in the following sections.

Overcoming constraints in a wireless communications system are paramount in achieving cohesive transmission required for the next generation of wireless communication systems. A technique that addresses these impediments by reducing the probability of occurrence of communication failures triggered by a phenomenon known as fading, and widely implemented, is the diversity technique. This technique provides the communication channel with numerous replicas of a signal over independently fading paths and received through multiple paths resulting in a reduction of the likelihood that all replicas of the signal will fade simultaneously [5], subsequently stabilizing the wireless link. The uncorrelated faded signals are collected from the diversity branches with combining techniques to get the benefits of improved error performance and signal-to-noise ratio (SNR) of radio channel without increasing the transmitted power. Diversity techniques are categorized as frequency, polarization, angle, antenna, time, space and signal space diversity [5]. The various diversity combining methods available are maximal ratio combining (MRC), Switched combining (SWC), selection combining (SC), equal gain combining (EGC), periodic switching method and phase sweeping method. MRC is the optimal combiner that improves the error performance of a communication system subjected to independent AWGN and fading amongst diversity branches.

Among the mentioned diversity techniques, spatial diversity (space diversity) is mostly preferred in wireless communication systems because it offers diversity without additional transmission time or bandwidth expenditure. The multiple-input multiple-output (MIMO) technology has been recognized as the elementary technique for achieving high data rates and improving link reliability [6]. It is also regarded as a critical technique to improve the spectral efficiency of future wireless systems which provides diversity gain, spatial gain, and interference reduction capability [7]. Furthermore, MIMO technology considerably increases the capacity of a given channel while conforming to Shannon's law. Moreover, the wireless IEEE 802.11n standard supports MIMO technology adopted by smart devices.

There are numerous ways of implementing MIMO systems to combat signal fading and improve the channel capacity. The use of space-time coding (STC) which is another form of transmit diversity, enables the establishment of additional spatial channels, thereby increasing achievable data rate and the system capacity. STC's employ redundancy to provide protection against noise, interference and channel fading. These STC's are classified into two categories as Space-Time Trellis Codes (STTC) and Space-Time Block Codes (STBC). The former coding technique relies on the trellis-coded modulation (TCM) scheme which is both a coding and modulation technique for digital transmission. STTC allows for serial transmission of symbols through linking signal processing at the receiver with coding techniques proper for use with multiple antennas at the transmitter while decoding of the symbols requires a multidimensional version of the Viterbi algorithm. Although STTC enhances coding gain, therefore, improving the error performance, it is at the expense of increased decoding complexity at the receiver due to the soft Viterbi decoder [8]. In

contrast, STBC transmission of the signal occurs in blocks. It is intended to realize a maximum diversity order for a specified quantity of transmitting and receiving antennas subject to the restriction of having a simple decoding algorithm.

An important and particularly simple STBC scheme developed by Alamouti [9], uses the complex orthogonal signal set. Although this orthogonal STBC does not provide a coding gain, it provides full diversity potential without sacrificing its data rate and has the advantage of the decoder simply requiring some linear combinations of the received symbol [10]. A wide range of transmission schemes has been proposed in the literature to enhance the spectral efficiency of Alamouti STBC. Of particular interest, it is Spatial Modulation (SM) scheme introduced in [11]. The introduction of SM to STBC exploits spatial multiplexing and subsequently enhances the spectral efficiency exemplified in STBC-SM scheme [6]. To meet the ever-growing demand for high data-rate transmissions, further enhancement of the spectral efficiency of these MIMO based schemes is required. A technique that expands the orthogonal STBC by the use of unitary matrix transformation in [12] has been explored. This approach improves the spectral efficiency of the orthogonal STBC scheme without increasing the size of the amplitude/phase modulation (APM) symbol set, thus preventing an increase in the peak-to-average power ratio (PAPR).

In this dissertation, we pay particular attention to improving the Spectral efficiency of the conventional STBC-SM system using the approach of expanding the STBC through the use of unitary matrix transformation which results in a system termed Enhanced spectral efficiency of STBC-SM (E-STBC-SM).

1.2 An overview of channel fading

In this section, the phenomenon of multipath propagation resulting in channel fading is discussed with mitigating techniques deployed in wireless communications to advance the reliability of the link.

1.2.1 Multipath Fading Channels

Radio channels such as ionospheric scatter and tropospheric scatter endure fading due to the aforementioned phenomenon where the radio signal may go through reflection, absorption, scattering and diffraction by signal obstructing objects between transmitter and receiver [13]. Transmitted signals reach the receiver via multiple independent paths and different time instances. Thus, each signal experiences independent attenuation and noise interference. The received signals are superimposed though some add destructively even resulting in phase shifting. The addition of these destructive signals is known as fading [13].

1.2.2 Rayleigh Fading Model

Rayleigh fading channel is a stochastic multipath fading used to model a rich scattering environment. It assumes that there is no line-of-sight (LOS) route between transmitter and receiver. Both the in-phase and quadrature components of the fading are modeled as independent and identically distributed (i.i.d.) Gaussian random variables where the fading coefficient is expressed as:

$$\alpha = a^I + ja^Q \quad (1.1)$$

where a^I and a^Q are the in-phase and quadrature components respectively and are Gaussian random variables (RV's) with zero mean and 0.5. The Rayleigh distributed fading amplitude is given by [14]:

$$A = \sqrt{|a^I|^2 + |a^Q|^2} \quad (1.2)$$

The probability density function (PDF) of the fading amplitude A is given by [14]:

$$f(A) = 2A \exp(-A^2), \quad A \geq 0 \quad (1.3)$$

In this dissertation, all fading cases are assumed to be Rayleigh frequency-flat fading.

1.3 An Outline of Diversity Techniques

Wireless communication uses numerous techniques to alleviate the effects of multipath fading classified as Diversity. The core of diversity is to receive multiple replicas of the transmitted signal experiencing independent fading and exploiting the probability that some of the received copies of the transmitted signal will be minimally attenuated than the probability of a single signal transmitted. Thus, these received signals are combined to accurately estimated the transmitted signal. Various diversity techniques are briefly discussed below.

1.3.1 Time

Time diversity is accomplished by transmitting the same signal several times using different time intervals resulting in uncorrelated fading signals at the receiver. The necessary time separation for transmission is the coherent time of the channel which is the statistical measure of the period time over which the channel fading process is correlated [15]. The time-varying nature of the wireless channel is exploited by employing symbol interleaving resulting in decoding delays. A trade-off between improved reliability and Spectral efficiency exists where the latter suffers [15].

1.3.2 Frequency

Frequency diversity is accomplished by the transmission of the same signal using multiple frequency bands experiencing uncorrelated fading scenarios. The frequencies need to be separated by the order of several times the channel coherence Spectral ensuring that the fading is essentially uncorrelated. Similar to time diversity, frequency diversity suffers an attenuation in Spectral efficiency owing to redundancy in the frequency domain [15].

1.2.3 Space

Space/Antenna diversity is a common technique in wireless communications. Unlike the two previous techniques, Antenna diversity does not suffer any loss in Spectral efficiency. Spatial locations of the transmit or receive antenna are physically separated a proper distance to avoid correlation, though a few wavelengths are adequate to attain uncorrelated signals [15]. The replicas of the transmitted signals are combined using one of the mentioned combining techniques at the receiver to increase the overall received SNR.

1.2.4 Signal Space

Signal space diversity (SSD) exploits the inherent diversity of signal constellation by performing constellation rotation in accordance to an optimum angle thus increasing the minimum number of distinct

components between any two constellation points [16]. The importance of rotation is to achieve the maximum number of distinct components in the new rotated signal constellation. To realize diversity in SSD, each signal point must have each component interleaved, therefore, ensuring that these components experience independent fading. SSD does not need any additional bandwidth, antennas or transmission power. However, SSD inherits a more complex maximum likelihood (ML) detector at the receive though needing additional processing power [16].

The Diversity techniques of interest in this dissertation are Space diversity and Time diversity as well as the MRC combining technique.

1.4 An Overview of Spectral Efficiency Enhancement Techniques

Spectral efficiency and Spectral efficiency improvement techniques employed in wireless communication systems particularly for STC's are briefly discussed in this section.

1.3.1 Spectral Efficiency

Normalized throughput, commonly branded as Spectral efficiency, is the rate of information transmitted per unit channel Spectral denoted in bits per second per Hz (b/s/Hz) [17]. There are two main factors that govern the Spectral efficiency of a wireless communication system namely; Modulation and coding scheme (MCS) such as M-ary quadrature amplitude modulation (M-QAM) and M-ary phase-shift keying (M-PSK), and SNR. The number of code bits that can be transmitted per modulated symbol is determined by the modulation order M expressed as $\log_2 M$ b/s/Hz [17]. The crest of Spectral efficiency improvement techniques is to enhance the efficiency beyond the general $\log_2 M$ b/s/Hz.

1.3.2 Spectral Efficiency Enhancement Techniques

The impediment of limited Spectral available in usable spectrum faced in the realm of wireless communication can be combated by employing Spectral efficiency improvement techniques to increase the rate of information transmitted over the Spectral hence allowing communication systems to accommodate more users or increase the data rate available to each user. These techniques can employ expanded space-time codes, expanded signal constellation or they can extend signals to the spatial domain in order to convey additional information. Narrowing this discussion to content related to this dissertation, space-time codes transmission schemes Spectral efficiency improvement techniques are briefly discussed below preceded by Space-time block codes.

1.3.2.1 Alamouti Space-time Block Codes

Exploiting the transmit diversity potential of a MIMO configuration is one attractive solution for achieving the required diversity order in receiver-constrained communication systems [18]. Alamouti [18] proposed a simple two-branch transmit diversity scheme for MIMO systems whereby two symbols are transmitted from two transmit antennas over two consecutive time slots. Alamouti STBC scheme with a 2×1 configuration is proficient of achieving the same diversity order as a 1×2 configuration conventional digital modulation technique with an MRC at the receiver. Alamouti suffers 3 dB loss in performance compared to MRC performance. This is due to the halving of the transmit power as a result of simultaneous data transmission [18]. Despite the performance loss related to STCs [19] and other transmit diversity MIMO schemes [19], Alamouti's STBC scheme remains an attractive solution for providing transmit diversity gains due to its simple implementation and low decoding complexity [20]. Furthermore, it is the only orthogonal STBC scheme which can achieve its full diversity potential without sacrificing its data rate [20]. In the subsequent sections, the Alamouti STBC scheme is presented.

1.3.2.2 Efficiency-Improved Alamouti Code

In [1], Ling *et al* proposed a coherent scheme termed efficiency-improved Alamouti (El-Alamouti) where multiple quadrature phase-shift keying (QPSK) signal constellations are utilized to enhance the Spectral efficiency of Alamouti STBC. The concept is, for a single additional bit, two distinct QPSK constellations are used. The second constellation is a rotated version of the first constellation which is the conventional QPSK constellation. Symbols in each transmitted block are taken from the same constellation, thus the El-Alamouti code preserves the full diversity of the conventional Alamouti STBC allowing the ML decoder to decouple symbols at the receiver. The selected constellation is a fixed function of the additional bit. Since El-Alamouti is a $2 \times N_r$ configured system, with a stream of bits of the size $n + 2 \log_2 M$ random bits fed into the El-Alamouti transmitter to select a pair of Gray-Coded MCS symbols from one of the 2^n constellations for transmission. When $n = 1$, an additional bit 0 selects the conventional QPSK constellation while bit 1 selects the rotated constellation.

Notation

Bold uppercase and lowercase letters are utilized for matrices and column vectors, respectively. $(\cdot)^*$, $(\cdot)^H$, $[\cdot]^T$, $(\cdot)^{-1}$ resemble complex conjugate, transpose conjugate of a matrix, transpose matrix and the inverse matrix respectively. $\operatorname{argmin}_x(f(x))$, $\operatorname{argmax}_x f(x)$ denote the argument of the minimum (argmin_x) and maximum (argmax_x) operator which returns a set of values of x for which function ($f(x)$) attains its smallest and largest value respectively. $|\cdot|$ and $\|\cdot\|_F$ represents the Euclidean norm and Frobenius norm respectively. $E\{\cdot\}$, $\binom{\cdot}{\cdot}$ and $\lfloor \alpha \rfloor_{2^p}$ represent statistical expectation, binomial coefficient, and the largest integer less than or equal to α , that is an integer power of 2, where p is an integer, respectively. Ω represents a complex signal constellation of size M .

1.5 The conventional MIMO system

MIMO systems overcome fading effects on the bases that the channels endure independent fading thus achieving improved Spectral efficiency, high data rates, and link reliability as a product of exploiting the potentials of spatial diversity [21]. MIMO technique is generally categorized into two classes of diversity and multiplexing schemes. The latter class is exemplified by the vertical-bell layered space-time (V-BLAST) system which allows for the simultaneous transmission of multiple independent data streams and yields high data rates. Moreover, schemes such as Alamouti which aid link reliability by transmitting multiple redundant replicas of data to a receiver over an independent channel encapsulates the broad class of diversity.

The downside of MIMO systems is the high dependence of the channel capacity gains on the transmit and receive antenna spacing [22], [23], antenna synchronization [24], [25], and the complex algorithms used to mitigate effects of inter-channel interference (ICI) at the receiver.

The underpinning concept of MIMO systems is characterized by establishing multiple channels founded on the usage of multiple antennas at the transmitter and receiver, thus increasing the effective channel capacity. Considering an $N_r \times N_t$ MIMO configured system, as demonstrated in Figure 1-1, where N_t and N_r represents the number of transmit and receive antennas respectively, with the system modelled as,

$$\mathbf{y} = \mathbf{H}\mathbf{x} + \mathbf{n} \quad (1.4)$$

where \mathbf{y} and \mathbf{n} denote the $N_r \times 1$ received signal and additive-white Gaussian noise (AWGN) vector, respectively. Furthermore, the $N_t \times 1$ transmit symbol vector \mathbf{x} and $N_r \times N_t$ channel matrix \mathbf{H} expressed as,

$$\mathbf{H} = \begin{bmatrix} h_{1,1} & \dots & h_{1,N_t} \\ \vdots & \ddots & \vdots \\ h_{N_r,1} & \dots & h_{N_r,N_t} \end{bmatrix} \quad (1.5)$$

where $h_{i,j}$ $i \in [1:N_r]$, $j \in [1:N_t]$ is the fading coefficient of the channel between i^{th} receive antenna and j^{th} transmit antenna. The entries in both \mathbf{H} and \mathbf{n} are assumed to be identically independently distributed (i.i.d.) random variables (RV) with distribution $\text{CN}\sim(0,1)$ and $\text{CN}\sim(0,1/\rho)$ respectively and ρ is the average SNR of the receive antenna.

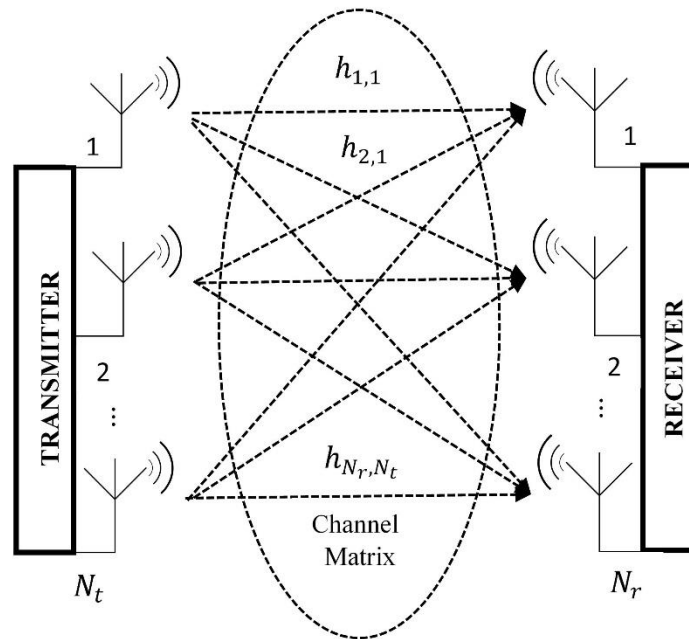


Figure 1-1: Demonstration of an $N_r \times N_t$ MIMO system

To exploit the MIMO systems, Space-time codes were designed. In so doing, the capacity of the wireless system increases enormously. These codes use an efficient way to allocate different symbols to different antennas while adding coding redundancy to minimize effects brought about fading. They can also achieve full antenna diversity and good coding gain [26]. In a bid to mitigate the aforementioned MIMO bottlenecks, Mesleh *et al.* [11] proposed a spatial multiplexing scheme named Spatial Modulation. These schemes are introduced and discussed in length in the subsequent section.

1.5.1 Space-Time Block Coded Spatial Modulation

MIMO systems, identified as a core technique for improving link reliability and attaining high data rate, have drawbacks where the capacity gains emanating from MIMO systems are greatly reliant on the transmit and receive antenna synchronization, antenna spacing, and algorithms used to reduce inter-channel interference at the receiver [27], thus enhanced error performance is realized at the expense of an increase in receiver complexity and cost [27]. The impairments were addressed by the introduction of spatial modulation (SM) which decreases the system complexity and cost while realizing high spectral efficiency and improved error performance. Spatial Modulation, introduced by [28], is a spatial multiplexing MIMO technique. It achieves high Spectral efficiency and overcomes ICI by triggering a single transmit antenna at each instant to transmit a certain data symbol where the index of the active antenna and data sent depends on incoming random bits [29]. One notable bottleneck of SM is the inability to exploit its potential for transmit diversity [30]. Basal *et al.* [6], merged the principles of SM and STBC in a way that the advantages of both are realized while circumventing their disadvantages in a scheme termed space-time block coded Spatial modulation (STBC-SM). This scheme exploits the transmit diversity potential of a MIMO configuration while circumventing ICI at the receiver [30]. Spectral efficiency of STBC-SM is $\frac{1}{2}\log_2 c + \log_2 M$ where c is the total number of antenna combinations and M is the modulation order. An optimal ML detector completely exploits the pros of Alamouti STBC-SM by execution a joint detection of modulated symbols and antenna indices over all possible cM^2 unique transmission matrices [6]. A simple near-maximum-likelihood low complexity detection scheme for Alamouti STBC-SM was proposed in [31] by Xu *et al.*, where the scheme achieved a very low computational complexity compared to the latter detection scheme and proved to be independent of the modulation size [31].

1.5.2 Space-Time Block Coded Spatial Modulation with Labelling Diversity

Labeling diversity is a scheme developed to improve the BER performance of bit-interleaved space-time block coded modulation. Termed space-time block coded spatial modulation with labeling diversity (STBC-SM-LD) [31], is a scheme that maintains the same structure to the conventional Alamouti STBC-SM whilst accomplishing a better BER performance as compared to the latter for the same Spectral efficiency. In the STBC-SM-LD scheme, a unique bit-to-constellation symbol mapper is employed for symbol transmitted in each of the two transmission slots [32], i.e. a mapped symbol pair is transmitted in the second time slot instead of a complex conjugate compared to the conventional STBC-SM scheme. The labeling maps and design methodology are discussed in length by Xu *et al.* [32]. As in [31], a shared detection of the modulated symbols and antenna indices is performed through a meticulous search over all possible cM^2 unique transmission matrices.

1.5.3 Super-orthogonal Space-Time Block Code Using a Unitary Expansion

This is a scheme that Improves error performance and Spectral efficiency with the means of expanding the orthogonal code using a unitary matrix transformation [12]. The objective in using Unitary matrix transformation is to have a higher spectral efficiency by increasing the cardinality of the STBC set. These matrices do not expand the resulting modulation signal constellation which avoids the undesirable escalation of the peak-to-average power ratio (PAPR) of the transmitted APM signal. For b additional bits per transmitted block to be conveyed, 2^b space-time signal set is required. However, certain considerations must be considered when designing of the unitary matrix such as Maximizing the minimum effective Hamming distance, minimum product measure, and minimum Euclidean distance to ensure that the increased rate does not affect the error performance of the super-orthogonal code.

Super-orthogonal STBC achieve both error performance and Spectral efficiency improvement particularly for a four transmit antenna STBC configuration at a cost of a slight complexity increase in the receiver. However, a two transmit antenna space-time code suffers from degradation in error performance which deteriorates further with an increase of the code rate [12].

1.6 Motivation and Contributions

1.6.1 Proposed Enhanced Spectral efficiency of M-PSK STBC-SM using unitary matrices

The unitary matrix transformation concept is employed to enhance the Spectral efficiency of space-time block code systems. Nonetheless, work in [12] shows degradation in BER performance for 2 transmit antennas when the rate is increased whilst enhancing Spectral efficiency of a coherent Alamouti scheme. To the best of the author's knowledge, a higher Spectral efficient space-time blocked coded spatial modulation system that retains the BER performance of conventional Alamouti STBC-SM scheme using unitary matrix transformation has not been reported in the literature.

Motivated by the above, the contributions are:

1. A Spectral efficiency enhancement technique for space-time block coded spatial modulation wireless communication system is explored and established named space-time block coded spatial modulation using unitary transformation matrix is proposed. Furthermore, the proposed system is shown to retain the BER performance of the conventional STBC-SM system with a maximum degradation of 3% in BER performance between modulation order 16,32 and 64.
2. A closed-form union bound expression to quantify the average BER performance of circular M-PSK STBC-SM using unitary expansion over independent and identically distributed (i.i.d.) Rayleigh frequency-flat fading channels is formulated.

1.7 Structure of the Dissertation

Chapter 2 presents a summary of MIMO and further details the system model of the conventional Alamouti STBC scheme. An analytical framework and Monte-Carlo simulations for average BER over Rayleigh frequency-flat fading channels of Alamouti STBC scheme are presented.

Chapter 3 presents a Spatial modulation scheme adopted for PSK. Monte-Carlo simulations are performed for average BER over Rayleigh frequency-flat fading channels and an Analytical framework is developed.

Chapter 4 details the STBC-SM scheme and formulates an analytical framework based on PSK modulator. Monte-Carlo simulations are developed for average BER over Rayleigh frequency-flat fading channels. Comparisons of SM and STBC-SM scheme are made under the same channel assumption.

Chapter 5 enhances the bandwidth efficiency of the Alamouti STBC-SM scheme (the proposed system is named Enhanced spectral efficiency of Alamouti STBC-SM (E-STBC-SM)). An analytical framework is developed and validation through Monte-Carlo simulations for average BER over Rayleigh frequency-flat fading channels is presented. Comparisons of the proposed scheme with conventional STBC-SM scheme are made.

Chapter 6 draws the conclusions of this dissertation, it summarizes the findings of this research and further proposes future research potentials.

Chapter 2

Alamouti space-time block coding

2.1. Introduction

The exploitation of diversity potential given by MIMO configuration is an attractive method that achieves diversity gain, coding gain and high spectral efficiency enabled with the introduction of Space-time coding by Tarokh *et al* [26]. Space coding is obtained by using multiple antennas at the transmitter where the ingenious coding of symbols across space and time is exploited to reap the benefits due to coding and diversity [33]. Designing of Space-time codes aim to optimize a trade-off between three incompatible objectives of maintaining a simple decoding algorithm, maximizing the information rate, and obtaining low error probability [9]. Another important property of Space-time code is its rate, defined as the ratio of the number of independent data symbols transmitted through the code matrix to the number of symbol time units that the code matrix spans. These codes can broadly be characterized as Space-Time block codes (STBC) and Space-Time trellis codes (STTC) where all these schemes aim to exploit redundancy to achieve high reliability, high spectral efficiency, and high-performance gain.

2.2. Space-time Block Coding

Space-time block coding is a technique that transmit multiple copies of a data stream through several antennas while exploiting the numerous received versions of the data to improve the reliability of data transfer. To achieve full diversity gain in this scheme, Alamouti pioneered a simple transmission diversity technique for systems with two transmit antennas [9]. This scheme termed Alamouti STBC was historically the first STBC scheme. It is a complex space-time diversity technique used in both MISO (multiple-in single-out) and MIMO configuration achieving full diversity gain without sacrificing its data rate.

2.3. Transmission

Alamouti proposed an STBC for two-branch transmits diversity incorporating two symbols periods represented by the coding matrix [18]:

$$\mathbf{X} = \begin{bmatrix} x_1 & x_2 \\ -x_2^* & x_1^* \end{bmatrix} \quad (2.1)$$

where $x_i \in \Omega, i \in [1:2]$, Ω is the set of quadrature amplitude modulation/phase shift keying (QAM/PSK) constellation with $E[|x_i|^2] = 1, i \in [1:2]$. The rows represent the first and second time slots and the columns show the first and second transmit antennas. Alamouti STBC is a rate-1 transmission scheme since two time-slots are needed to transmit both symbols. The system model of Alamouti STBC is shown in Figure2-1. The received signals can be denoted by

$$\mathbf{Y} = \mathbf{H}\mathbf{X} + \mathbf{N} \quad (2.2)$$

where \mathbf{Y} is the $2N_r \times 1$ received vector, $\mathbf{H} = [\mathbf{h}_1 \quad \mathbf{h}_2]$ is an $N_r \times 2$ channel matrix. $\mathbf{h}_i = [h_{i,1} \quad \dots \quad h_{i,j}]$ is assumed that the element $h_{i,j}$ of \mathbf{h}_i is the quasi-static Rayleigh frequency flat fading channel between the i^{th} receive antenna and j^{th} transmit antenna, $i \in [1:N_r], j \in [1:N_t]$. $h_{i,j}$ remains constant over two consecutive symbol intervals and takes another value over another two consecutive symbol intervals. $\mathbf{N} = [\mathbf{n}_1 \quad \dots \quad \mathbf{n}_i]^T$ is the $2N_r \times 1$ additive Gaussian noise (AWGN) vector. The entries in both \mathbf{H} and \mathbf{N} are assumed to be identically independently distributed (i.i.d.) random variables (RV) with distribution $\mathbb{CN}\sim(0,1)$ and $\mathbb{CN}\sim(0,2/\rho)$ respectively and ρ is the average SNR in each antenna at the receiver.

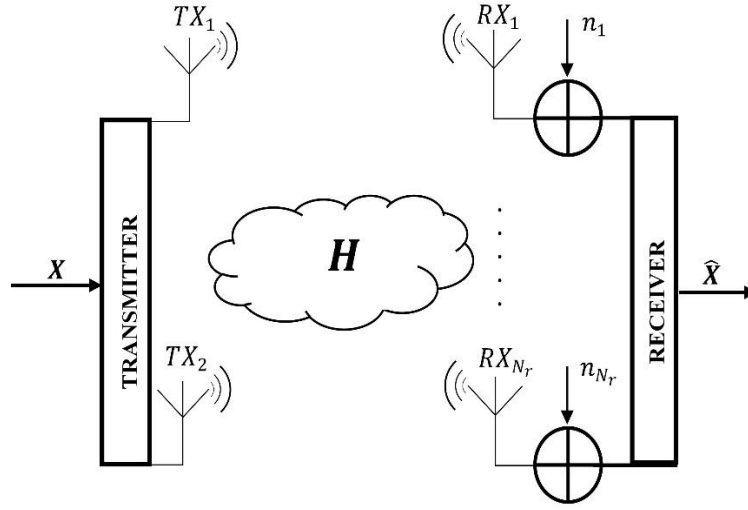


Figure 2-1: $N_r \times 2$ Alamouti STBC

Considering an $N_r \times 2$ Alamouti STBC system where one transmission interval is divided into two consecutive time slots. The first time-slot transmits symbols x_1 and x_2 through antenna 1 and antenna 2 respectively, while symbols $-x_2^*$ and x_1^* are transmitted through antenna 1 and antenna 2 respectively at the consecutive time-slot. The received signals $\mathbf{Y} = [\mathbf{y}_1 \ \mathbf{y}_2]^T$ are given by;

$$\begin{aligned}
 \text{Time slot 1:} \quad & \mathbf{y}_1 = \mathbf{h}_1 x_1 + \mathbf{h}_2 x_2 + \mathbf{n}_1 \\
 \text{Time slot 2:} \quad & \mathbf{y}_2 = -\mathbf{h}_1 x_2^* + \mathbf{h}_2 x_1^* + \mathbf{n}_2
 \end{aligned} \tag{2.3}$$

With the receiver having the perfect channel state information (CSI), the received signal is manipulated, thus yields

$$\tilde{\mathbf{Y}} = \begin{bmatrix} \mathbf{y}_1 \\ \mathbf{y}_2^* \end{bmatrix} = \begin{bmatrix} \mathbf{h}_1 & \mathbf{h}_2 \\ \mathbf{h}_2^* & -\mathbf{h}_1^* \end{bmatrix} \begin{bmatrix} x_1 \\ x_2 \end{bmatrix} + \begin{bmatrix} \mathbf{n}_1 \\ \mathbf{n}_2^* \end{bmatrix} \tag{2.4}$$

Let $\mathbf{H}_{eff} = \begin{bmatrix} \mathbf{h}_1 & \mathbf{h}_2 \\ \mathbf{h}_2^* & -\mathbf{h}_1^* \end{bmatrix}$ be the effective channel matrix. The received signals (2.4) are then combined (2.5) by multiplying both sides of the received signal with the Hermitian transposition of the effective matrix \mathbf{H}_{eff}^H [9].

$$\mathbf{z} = \begin{bmatrix} z_1 \\ z_2 \end{bmatrix} = \mathbf{H}_{eff}^H \tilde{\mathbf{Y}} = \begin{bmatrix} (\|\mathbf{h}_1\|^2 + \|\mathbf{h}_2\|^2)x_1 + \hat{n}_1 \\ (\|\mathbf{h}_1\|^2 + \|\mathbf{h}_2\|^2)x_2 + \hat{n}_2 \end{bmatrix} \quad (2.5)$$

where $\hat{n}_1 = \mathbf{h}_1^H \mathbf{n}_1 + \mathbf{n}_2^H \mathbf{h}_2$ and $\hat{n}_2 = -\mathbf{n}_2^H \mathbf{h}_1 + \mathbf{h}_2^H \mathbf{n}_1$. The effective channel matrix, \mathbf{H}_{eff} , is orthogonal such that $\mathbf{H}_{eff}^H \mathbf{H}_{eff} = \|\mathbf{H}\|_F^2 I_2$, where I_2 is the 2×2 identity matrix. The orthogonality of the effective channel matrix is that it permits for the transmitted symbols to be decoupled easily at the receiver by the use of simple linear processing. Moreover, the orthogonality of \mathbf{H}_{eff} also ensures that the elements of the noise vector, \mathbf{N} , are zero mean Circularly Symmetric complex Gaussian; therefore, independent optimal ML detection can be implemented for each transmitted symbol [34].

2.4. Detection

Decomposing (2.5) where z_1 and z_2 are given by;

$$\begin{aligned} z_1 &= \mathbf{h}_1^H \mathbf{y}_1 + \mathbf{y}_2^H \mathbf{h}_2 = (\|\mathbf{h}_1\|^2 + \|\mathbf{h}_2\|^2)x_1 + \mathbf{h}_1^H \mathbf{n}_1 + \mathbf{n}_2^H \mathbf{h}_2 \\ z_2 &= \mathbf{h}_2^H \mathbf{y}_1 - \mathbf{y}_2^H \mathbf{h}_1 = (\|\mathbf{h}_1\|^2 + \|\mathbf{h}_2\|^2)x_2 - \mathbf{n}_2^H \mathbf{h}_1 + \mathbf{h}_2^H \mathbf{n}_1 \end{aligned} \quad (2.6)$$

Due to the orthogonal nature of the Alamouti code, the symbols are equalized as

$$\begin{aligned} \tilde{x}_1 &= \frac{z_1}{(\|\mathbf{h}_1\|^2 + \|\mathbf{h}_2\|^2)} + \frac{\hat{n}_1}{(\|\mathbf{h}_1\|^2 + \|\mathbf{h}_2\|^2)} = x_1 + \tilde{n}_1 \\ \tilde{x}_2 &= \frac{z_2}{(\|\mathbf{h}_1\|^2 + \|\mathbf{h}_2\|^2)} + \frac{\hat{n}_2}{(\|\mathbf{h}_1\|^2 + \|\mathbf{h}_2\|^2)} = x_2 + \tilde{n}_2 \end{aligned} \quad (2.7)$$

The equalized signals are fed to the ML detector determining the estimates \hat{x}_1 and \hat{x}_2 of the transmitted symbols x_1 and x_2 . The decoding rules are therefore based on the minimization of the square Euclidean distance metric given by

$$\begin{aligned}\hat{x}_1 &= \arg \min_{x_1 \in \Omega} [|\tilde{x}_1 - x_1|^2] \\ \hat{x}_2 &= \arg \min_{x_2 \in \Omega} [|\tilde{x}_2 - x_2|^2]\end{aligned}\quad (2.8)$$

Furthermore, Alamouti revealed that the two-branch scheme can be extended to cater for receive diversity using multiple receive antenna configuration.

The transmit power is equally shared by the simultaneously transmitting antennas.

2.5. BER Performance Analysis

Alamouti STBC scheme showed that with two transmit antennas and N_r receive antennas, it is equivalent to the maximum ratio combining (MRC) system with one transmit and $2N_r$ receive antennas though suffering a 3 dB loss due to halved power on each of the transmit antennas. Therefore, the closed form expression for the average BER of an $2 \times N_r$ M-QAM Alamouti STBC scheme over i.i.d. Rayleigh frequency-flat fading channels is given as [31, eq. 19]:

$$\begin{aligned}P_{d_{QAM}} &= \frac{a}{mn} \left\{ \frac{1}{2} \left(\frac{2}{b\rho + 1} \right)^{2N_r} - \frac{a}{2} \left(\frac{1}{b\rho + 1} \right)^{2N_r} + (1 - a) \sum_{k=1}^{n-1} \left(\frac{S_k}{b\rho + S_k} \right)^{2N_r} \right. \\ &\quad \left. + \sum_{k=1}^{2n-1} \left(\frac{S_k}{b\rho + S_k} \right)^{2N_r} \right\}\end{aligned}\quad (2.9)$$

where $a = \left(1 - \frac{1}{\sqrt{M}}\right)$, $b = \frac{3}{M-1}$, $m = \log_2 M$, n is the number of iterations for convergence, ρ represents the average SNR at each receive antenna and $S_k = 2 \sin^2 \left(\frac{k\pi}{2n}\right)$.

For M-PSK Alamouti STBC scheme, the average BER is given as [25]:

$$P_{d_{PSK}} = \frac{M-1}{Mmn} \left[\frac{1}{2} \left(\frac{\sin^2 \theta}{\sin^2 \theta + \rho \sin^2 \beta} \right)^{2N_r} + \sum_{k=1}^{n-1} \left(\frac{\sin^2 \frac{k\theta}{n}}{\sin^2 \frac{k\theta}{n} + \rho \sin^2 \beta} \right)^{2N_r} \right] \quad (2.10)$$

where $\theta = \pi - \beta$, $\beta = \pi/M$.

2.6. Results

This section presents simulation and analytical outcomes for Alamouti STBC scheme with different receive antenna configuration, i.e. $N_r \in [1:2]$. Comparison in BER vs SNR between SISO and MRC scheme are then presented. These comparisons we made with the following configurations:

- i. 2×1 : 16-PSK STBC vs 2×2 : 16-PSK STBC vs 1×1 : 16-PSK
- ii. 2×1 : 16-PSK STBC vs 1×2 : 16-PSK MRC
- iii. 2×2 : 16-PSK STBC vs 1×4 : 16-PSK MRC

The analytical framework developed in the preceding Section 2.5 are validated with Monte-Carlo simulations achieved over i.i.d. Rayleigh frequency-flat fast fading channels illustrated in Figure 2-3 and Figure 2-4. The evaluations are made at BER value of 10^{-6} .

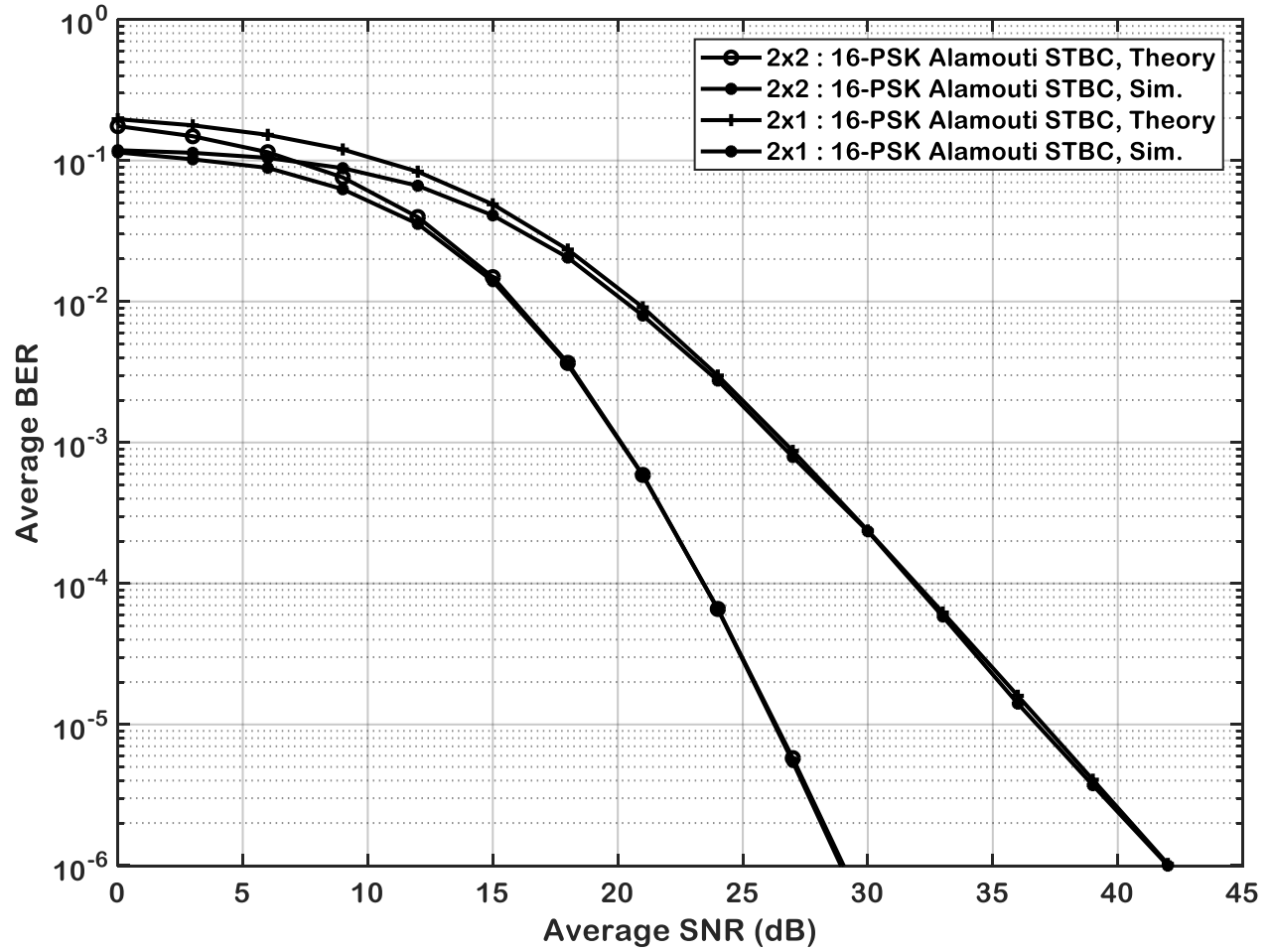


Figure 2-2: M-PSK Alamouti STBC Analytical and Monte-Carlo simulations

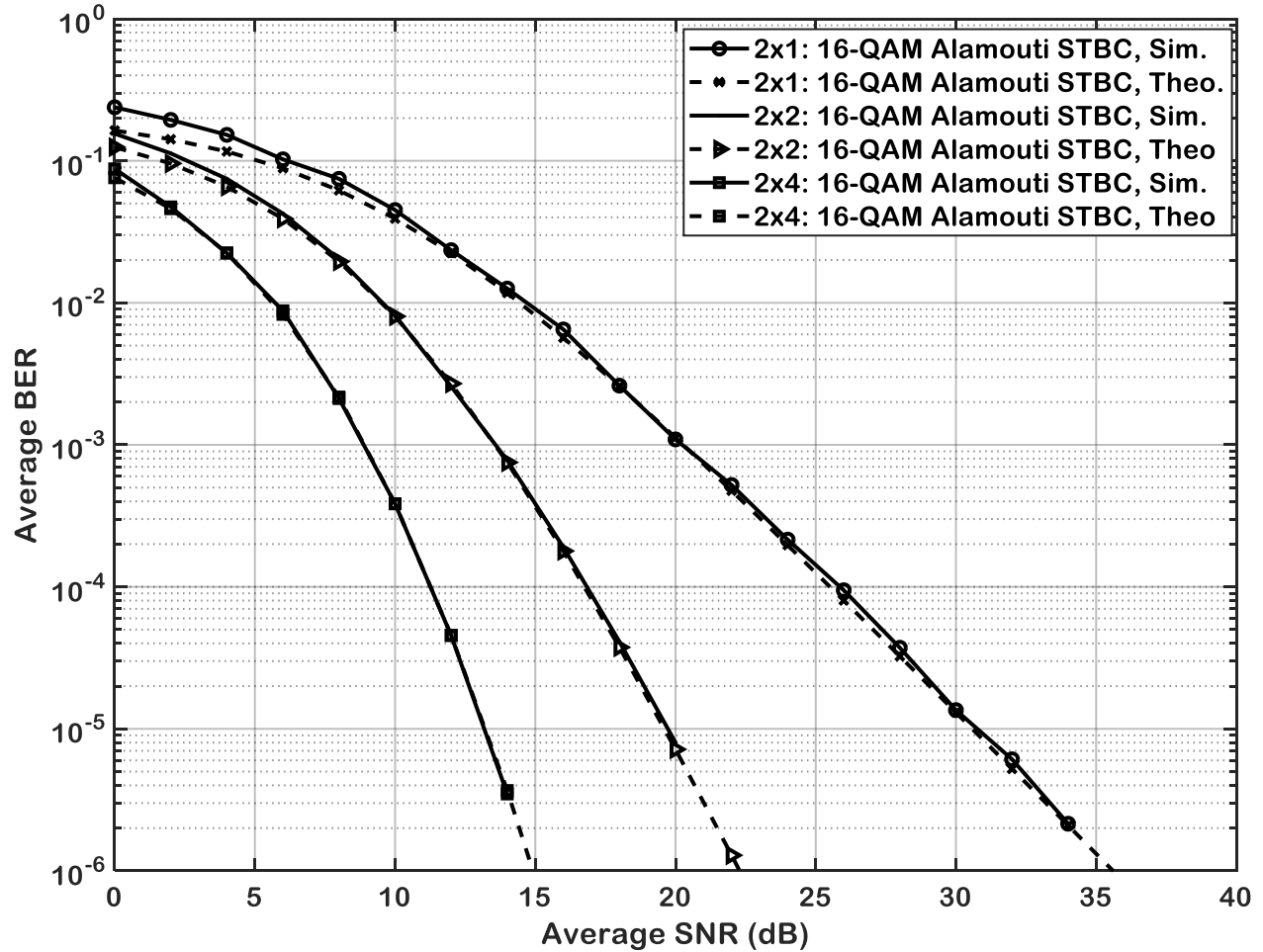


Figure 2-3: M-QAM Alamouti STBC Analytical and Monte-Carlo simulations

2.6.1. 16-PSK with MRC vs 16-PSK ALAMOUTI STBC

A comparison between maximum ratio combining and Alamouti STBC with 16-PSK as the digital modulation scheme. The comparing criterion is diversity gain of the order 2 and 4. In obtaining a diversity gain of 2, MRC was configured as a $N_t = 2, N_r = 1$ system exemplifying transmit diversity. Alamouti STBC was set-up for receive diversity with configurations $N_t = 1, N_r = 2$. In diversity gain of 4, MRC had $N_t = 4, N_r = 1$ and Alamouti STBC had $N_t = 2, N_r = 2$ configurations.

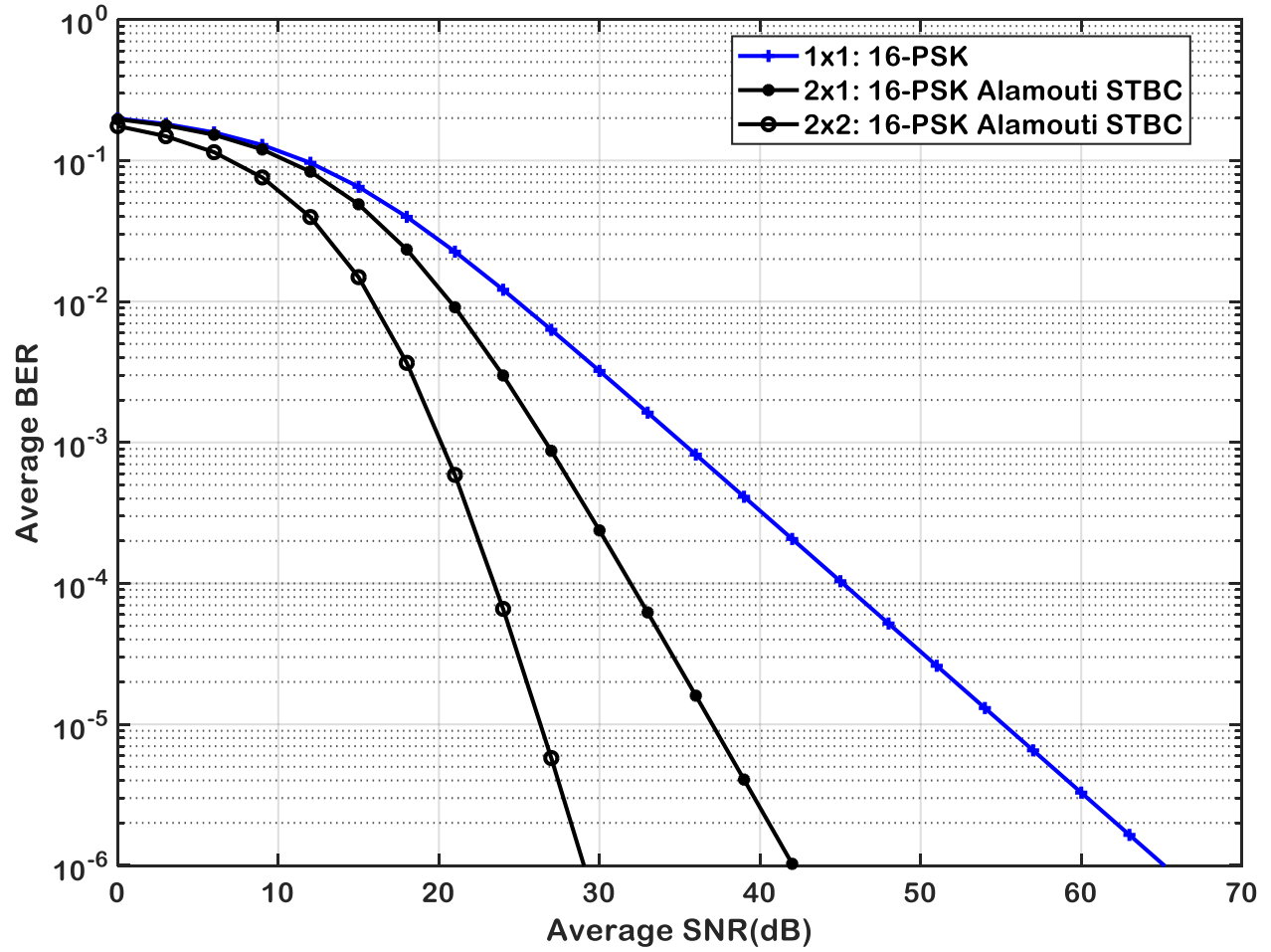


Figure 2-4: Comparison of $2 \times N_r$ 16-PSK Alamouti STBC Vs 16-PSK SISO scheme

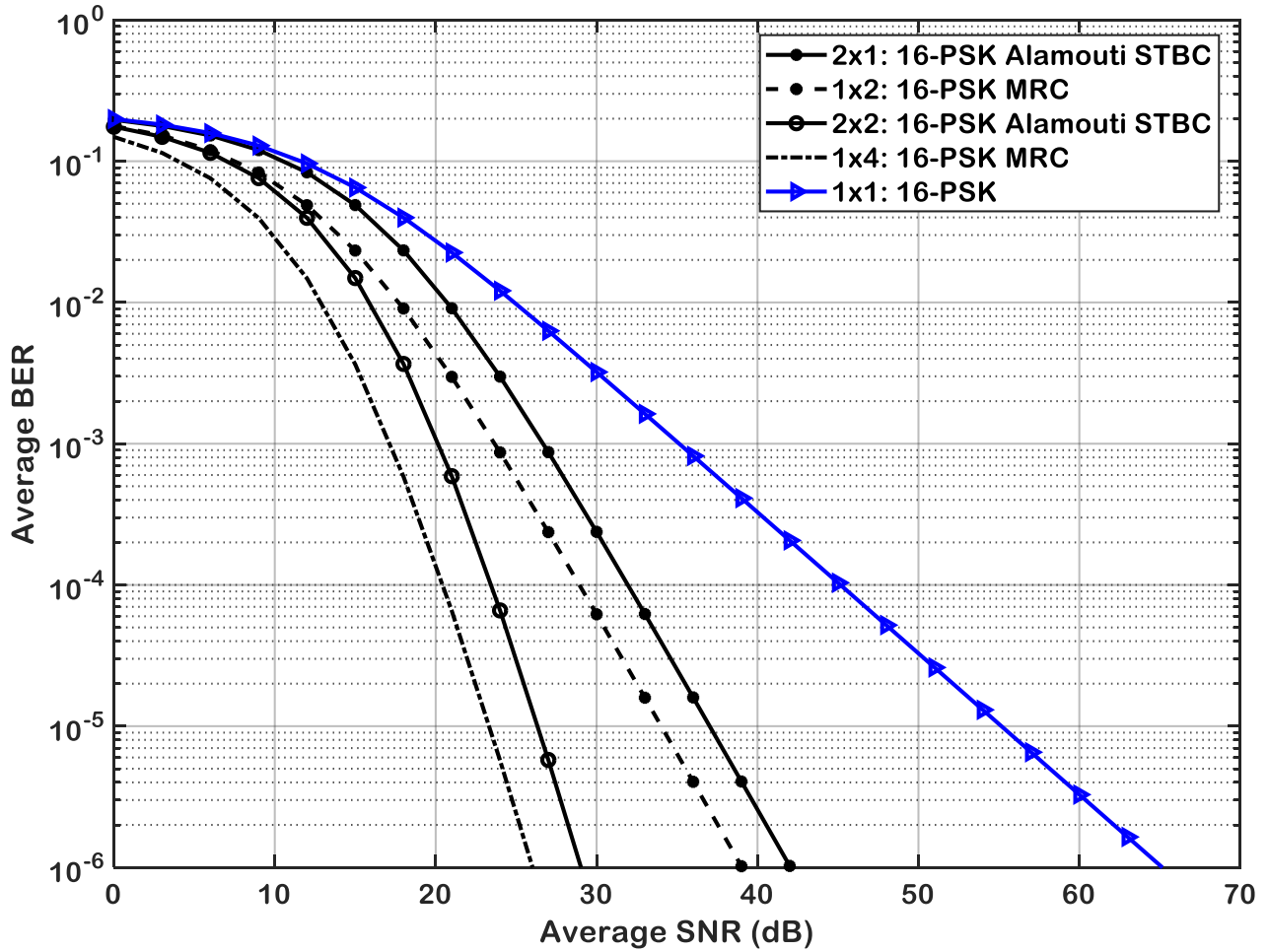


Figure 2-5: Comparison of 16-PSK Alamouti STBC Schemes with MRC and SISO schemes

As per expected, the Alamouti STBC scheme had a degradation in error performance of 3dB in signal-to-noise ratio for both configurations against MRC owing to the halved transmit power on each of the two transmit antennas. Furthermore, it was observed that the Alamouti scheme using two transmit antennas and N_r receive antennas has a diversity order of $2N_r$. The error performance improved significantly with the introduction of either transmit or receive diversity over a SISO scheme. Monte-Carlo simulations demonstrating the above discussion are illustrated in Figure 2-6.

2.7. Chapter synopsis and Conclusions

Alamouti STBC exhibits a substantial improvement in BER performance relative to a SISO scheme. These Alamouti schemes achieve full diversity gain without sacrificing its data rate. For both $N_t = 2, N_r = 1$ and $N_t = 2, N_r = 2$ configurations, Alamouti schemes are proficient of achieving identical diversity order as that of $N_t = 1, N_r = 2$ and $N_t = 1, N_r = 4$ antenna configurations using the conventional digital modulation technique with MRC reception respectively. Nonetheless, Alamouti suffers from a 3 dB degradation in performance relative to MRC systems compared with the same diversity order. As discussed early, this is brought about by the halving of the transmit power of each Alamouti STBC schemes transmitting antennae.

Furthermore, A $N_t = 2, N_r = 2$ configured Alamouti scheme which exploits both transmit and receive diversity provides improved BER performance brought about by the effective channel information from the 2 receive antennae over 2 symbols resulting in a diversity order of 4. Generally, Alamouti schemes with N_r receive antennae have a diversity order of $2N_r$.

Chapter 3

Spatial Modulation

3.1. Introduction

The introduction of a third-dimensional signal plane which is the spatial (antenna) dimension by Mesleh et al. in [28] named spatial modulation, to the traditional 2-D of MIMO schemes is an ingenious method in exploiting spatial multiplexing. This form of spatial multiplexing avoids bottlenecks such as transmit antenna synchronization and algorithms used to completely remove ICI at the receiver caused by transmitting simultaneously with all antennas exemplified by V-BLAST transmit scheme.

In a nutshell, Spatial modulation is a low complexity multiple-input multiple-output (LC MIMO) transmission technique that improves spectral efficiency by exploiting the spatial domain of the transmit antennas. This leads to information being conveyed not only by the APM techniques such as M-QAM and M-PSK also by active antenna indices. Moreover, since only a single active antenna is used to convey information at a particular time slot, the system is more energy-efficient.

3.2 Transmission

The conventional SM is an $N_r \times N_t$ scheme with N_t an integer power of two, where N_t and N_r denote the number of transmit and receive antennas respectively.

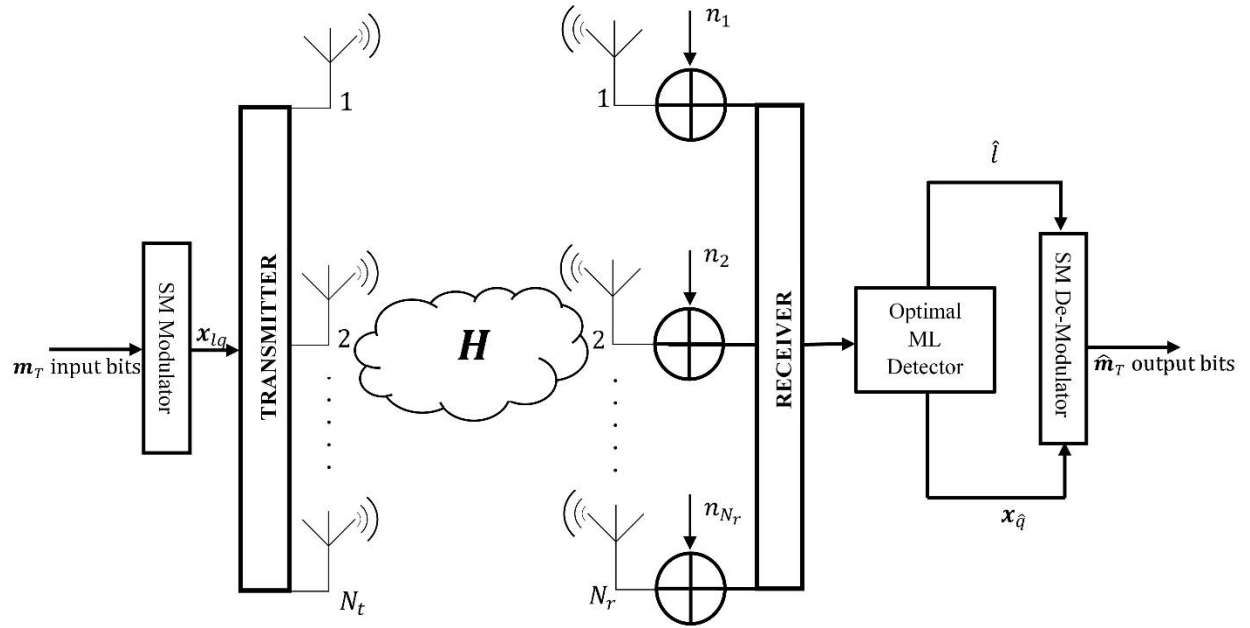


Figure 3-1: $N_r \times N_t$ SM System model

Considering an $N_r \times N_t$ SM-MIMO system, where the transmitted signal vector is

$$\mathbf{x}_{lq} = \begin{matrix} & & l^{\text{th}} \text{ position} & & \\ & & \downarrow & & \\ & & [0 \ 0 \ \dots \ x_q \ \dots \ 0]^T & & \\ & \uparrow & & \uparrow & \\ 1^{\text{st}} \text{ position} & & & & N_t^{\text{th}} \text{ position} \end{matrix} \quad (3.1)$$

$l \in [1:N_t]$ represents the transmitted symbol on the l^{th} antenna over the channel \mathbf{H} of i.i.d. random variable having dimension $N_r \times N_t$. A single non-zero element of \mathbf{x}_{lq} exists on the active antenna while the remainder of the elements is zero. Hence, this scheme can transmit $\log_2(N_t M)$ bits in each slot [35]. The system model of this SM scheme is illustrated in Figure 3-1. x_q resembles the q^{th} symbol from the M-PSK/M-QAM cardinality of the signal constellation diagram, with unit average power, i.e. $E[|x_q|^2] = 1$.

Table 3-1: Gray-coded constellation points for 8-PSK-SM modulation order

Input Bits	Antenna index l	Symbol x_q	Transmitted signal x_{lq}
00000	[00] = 1	[000] = $1 + j0$	$[1 + j0 \ 0 \ 0 \ 0]^T$
00001	[00] = 1	[001] = $0.7071 + j 0.7071$	$[0.7071 + j 0.7071 \ 0 \ 0 \ 0]^T$
00010	[00] = 1	[010] = $-0.7071 + j 0.7071$	$[-0.7071 + j 0.7071 \ 0 \ 0 \ 0]^T$
00011	[00] = 1	[011] = $0 + j 1$	$[0 + j 1 \ 0 \ 0 \ 0]^T$
00100	[00] = 1	[100] = $0.7071 - j 0.7071$	$[0.7071 - j 0.7071 \ 0 \ 0 \ 0]^T$
00101	[00] = 1	[101] = $0 - j 1$	$[0 - j 1 \ 0 \ 0 \ 0]^T$
00110	[00] = 1	[110] = $-1 + j 0$	$[-1 + j 0 \ 0 \ 0 \ 0]^T$
00111	[00] = 1	[111] = $-0.7071 - j 0.7071$	$[-0.7071 - j 0.7071 \ 0 \ 0 \ 0]^T$
01000	[01] = 2	[000] = $1 + j0$	$[0 \ 1 + j0 \ 0 \ 0]^T$
01001	[01] = 2	[001] = $0.7071 + j 0.7071$	$[0 \ 0.7071 + j 0.7071 \ 0 \ 0]^T$
01010	[01] = 2	[010] = $-0.7071 + j 0.7071$	$[0 \ -0.7071 + j 0.7071 \ 0 \ 0]^T$
01011	[01] = 2	[011] = $0 + j 1$	$[0 \ 0 + j 1 \ 0 \ 0]^T$
01100	[01] = 2	[100] = $0.7071 - j 0.7071$	$[0 \ 0.7071 - j 0.7071 \ 0 \ 0]^T$
01101	[01] = 2	[101] = $0 - j 1$	$[0 \ 0 - j 1 \ 0 \ 0]^T$
01110	[01] = 2	[110] = $-1 + j 0$	$[0 \ -1 + j 0 \ 0 \ 0]^T$
01111	[01] = 2	[111] = $-0.7071 - j 0.7071$	$[0 \ -0.7071 - j 0.7071 \ 0 \ 0]^T$
10000	[10] = 3	[000] = $1 + j0$	$[0 \ 0 \ 1 + j0 \ 0]^T$
10001	[10] = 3	[001] = $0.7071 + j 0.7071$	$[0 \ 0 \ 0 \ 0.7071 + j 0.7071 \ 0]^T$
10010	[10] = 3	[010] = $-0.7071 + j 0.7071$	$[0 \ 0 \ -0.7071 + j 0.7071 \ 0]^T$
10011	[10] = 3	[011] = $0 + j 1$	$[0 \ 0 \ 0 + j 1 \ 0]^T$

10100	[10] = 3	[100] = 0.7071 - j 0.7071	[0 0 0.7071 - j 0.7071 0] ^T
10101	[10] = 3	[101] = 0 - j 1	[0 0 0 - j 1 0] ^T
10110	[10] = 3	[110] = -1 + j 0	[0 0 -1 + j 0 0] ^T
10111	[10] = 3	[111] = -0.7071 - j 0.7071	[0 0 1 + j 0 0] ^T
11000	[11] = 4	[000] = 1 + j 0	[0 0 0 0.7071 + j 0.7071] ^T
11001	[11] = 4	[001] = 0.7071 + j 0.7071	[0 0 0 -0.7071 + j 0.7071] ^T
11010	[11] = 4	[010] = -0.7071 + j 0.7071	[0 0 0 0 + j 1] ^T
11011	[11] = 4	[011] = 0 + j 1	[0 0 0 0.7071 - j 0.7071] ^T
11100	[11] = 4	[100] = 0.7071 - j 0.7071	[0 0 0 0 - j 1] ^T
11101	[11] = 4	[101] = 0 - j 1	[0 0 0 -1 + j] ^T
11110	[11] = 4	[110] = -1 + j 0	[0 0 0 -0.7071 - j 0.7071] ^T
11111	[11] = 4	[111] = -0.7071 - j 0.7071	[0 0 0 1 + j 0] ^T

As an example, a 4×4 8-PSK-SM configured system is considered in Table 3-1. The first two bits from the MSB activates the antenna index l and the last three bits selects the symbol x_q from the PSK symbol set. The bits that are mapped are then transmitted through the single transmit antenna l activated by the antenna index.

The vector of the received signal is expressed in equation (3.2) as

$$\mathbf{y} = \mathbf{H}\mathbf{x}_{lq} + \mathbf{n} \quad (3.2)$$

where $\mathbf{y} = [y_1 \ y_2 \ \dots \ y_{N_r}]^T$ is an $N_r \times 1$ received signal, \mathbf{H} is an $N_r \times N_t$ dimensional Rayleigh frequency-flat fading channel vector assumed to be constant over the symbol period where $\mathbf{H} = [\mathbf{h}_1 \ \mathbf{h}_2 \ \dots \ \mathbf{h}_{N_t}]$. Each vector $\mathbf{h}_i, i \in [1:N_t]$ is given as $\mathbf{h}_i = [h_1 \ \dots \ h_j]^T$ and assumed that the element h_j of \mathbf{h}_i is the Rayleigh fading channel between the i^{th} transmit antenna and j^{th} receive antenna, $i \in [1:N_t], j \in [1:N_r]$. $\mathbf{n} = [n_1 \ n_2 \ \dots \ n_{N_r}]^T$ is the additive Gaussian noise (AWGN) with $N_r \times 1$

dimension. The assumption being that both entries of \mathbf{H} and \mathbf{n} are identically independently distributed random variables with distribution $\mathbb{CN}\sim(0,1)$ and $\mathbb{CN}\sim(0,1/\rho)$ respectively. Since the information symbols are modulated onto two information-carrying units a). One PSK/QAM symbol and b). a single active transmit antenna, the spectral efficiency is then given as

$$\eta_{SM} = \log_2 N_t + \log_2 M \quad (3.3)$$

where M is the modulation order.

3.3. Spatial Modulation Detection

The assumption is that the channel state information (CSI) is known at the receiver. Hence, an optimal detector based on the ML principle is used where the need for constrained channels is not necessitated. The receiver, with the use of the ML, executes a combined estimation of the transmit antenna index and symbol. Based on the received signal in (3.2) the detection rule is applied as follows [36, Eq. (4)]

$$\begin{aligned} [\hat{l}, x_{\hat{q}}] &= \underset{l,q}{\operatorname{argmax}} P_{\gamma}(\mathbf{y}|\mathbf{x}_{lq}, \mathbf{H}) \\ &= \underset{l,q}{\operatorname{argmin}} [\|\mathbf{g}\|_F^2 - 2\operatorname{Re}\{\mathbf{y}^H \mathbf{g}\}] \end{aligned} \quad (3.4)$$

where $l \in [1:N_t]$, $q \in [1:M]$ and $\mathbf{g} = \mathbf{H}\mathbf{x}_{lq}$. $P_{\gamma}(\mathbf{y}|\mathbf{x}_{lq}, \mathbf{H}) = \pi^{-N_r} \exp(-\|\mathbf{y} - \mathbf{H}\mathbf{x}_{lq}\|_F^2)$ is the probability density function (PDF) of the received signal vector \mathbf{y} conditioned on both \mathbf{x}_{lq} and \mathbf{H} . \hat{l} and $x_{\hat{q}}$ resemble the probable transmit antenna index and symbol index respectively.

3.4. Performance Analysis

This section encapsulates a derivation of an asymptotic error performance bound for M-PSK/M-QAM SM with optimal detection in i.i.d. Rayleigh flat fading channel conditions. Since spatial modulation considers multiple transmit antennas as additional constellation points and maps, the first part of a block of information bits to the transmit antenna indices and the second part of the block of information bits are mapped to a complex symbol using APM schemes [37], the bit error probability (BEP) performance of SM is reliant on the probability error of both antenna and symbol mapping process. The estimation processes of the transmit antenna pair index and symbol were assumed to be independent, hence the overall BEP is given by (3.5) [38],

$$P_e \geq P_a + P_d - (P_a P_d) \quad (3.5)$$

where P_a is the BEP (bit error probability) of incorrectly estimation the transmit antenna index assuming that the transmitted symbol is detected correctly and P_d is the probability of error due to incorrect estimation of the transmitted symbol assuming that the transmit antenna index is detected correctly. In this thesis $P_a = P_{d_{QAM}}$ for MQAM while $P_a = P_{d_{PSK}}$ for MPSK.

The average BEP for square M-QAM over Rayleigh fading channel is defined as [39, Eq. (13)]

$$P_{d_{QAM}} = \frac{a}{mn} \left\{ \frac{1}{2} \left(\frac{2}{b\rho + 1} \right)^{N_r} - \frac{a}{2} \left(\frac{1}{b\rho + 1} \right)^{N_r} + (1 - a) \sum_{k=1}^{n-1} \left(\frac{S_k}{b\rho + S_k} \right)^{N_r} + \sum_{k=1}^{2n-1} \left(\frac{S_k}{b\rho + S_k} \right)^{N_r} \right\} \quad (3.6)$$

where $a = \left(1 - \frac{1}{\sqrt{M}}\right)$, $b = \frac{3}{M-1}$, $m = \log_2 M$, n represent the number of iterations for convergence and $S_k = 2 \sin^2 \left(\frac{k\pi}{4n} \right)$.

The analytical BEP of the estimated symbol for M-PSK over Rayleigh fading channel has been derived and defined as [25],

$$P_{d_{PSK}} = \frac{M-1}{Mmn} \left[\frac{1}{2} \left(\frac{\sin^2 \theta}{\sin^2 \theta + \rho \sin^2 \beta} \right)^{N_r} + \sum_{k=1}^{n-1} \left(\frac{\sin^2 \frac{k\theta}{n}}{\sin^2 \frac{k\theta}{n} + \rho \sin^2 \beta} \right)^{N_r} \right] \quad (3.7)$$

where $\theta = \pi - \beta$, $\beta = \frac{\pi}{M}$, M is the symbol constellation size, ρ is the scaled average SNR at each receive antenna and n is the number of iterations greater than 10.

In deriving the analytical BER of the transmit antenna index, the approach in [36], [41] was followed. Assuming that the symbol transmitted is correctly detected, the average BEP of transmit antenna index estimation is union bounded in [38, (13)], as:

$$P_a \leq \sum_{q=1}^M \sum_{l=1}^{N_t} \sum_{\hat{l}=1}^{N_t} \frac{N(l, \hat{l}) \mu_\alpha^{N_r} \sum_{w=0}^{N_r-1} \binom{N_r-1+w}{w} [1-\mu_\alpha]^w}{N_t M} \quad (3.9)$$

where $\mu_\alpha = \frac{1}{2} \left(1 - \sqrt{\frac{\sigma_\alpha^2}{1+\sigma_\alpha^2}} \right)$, $\sigma_\alpha^2 = \frac{\rho}{2} |x_q|^2$, $q \in [1 : M]$ and $N(l, \hat{l})$ is the number of bits in error between transmitted transmit antenna index l and estimated phase index \hat{l} .

3.5. Analytical and Simulation Results

This section presents simulation and analytical outcomes for SM scheme. The comparisons are based on the throughput of 5 bpcu systems with the following configurations:

- i. 2×2 : 16-PSK SM
- ii. 4×4 : 8-PSK SM vs 4×4 : 16-PSK SM
- iii. 4×4 : 4-QAM SM vs 4×4 : 16-QAM SM

The analytical framework illustrated in Section 3.4 is validated with Monte Carlo simulations performed over i.i.d. Rayleigh flat fading channels. Evaluations are made at BER value of 10^{-5} with the assumption that: full knowledge of the channel is available at the receiver; the transmit and receive antennas are spaced to circumvent correlation and MRC reception is utilized at the receiver.

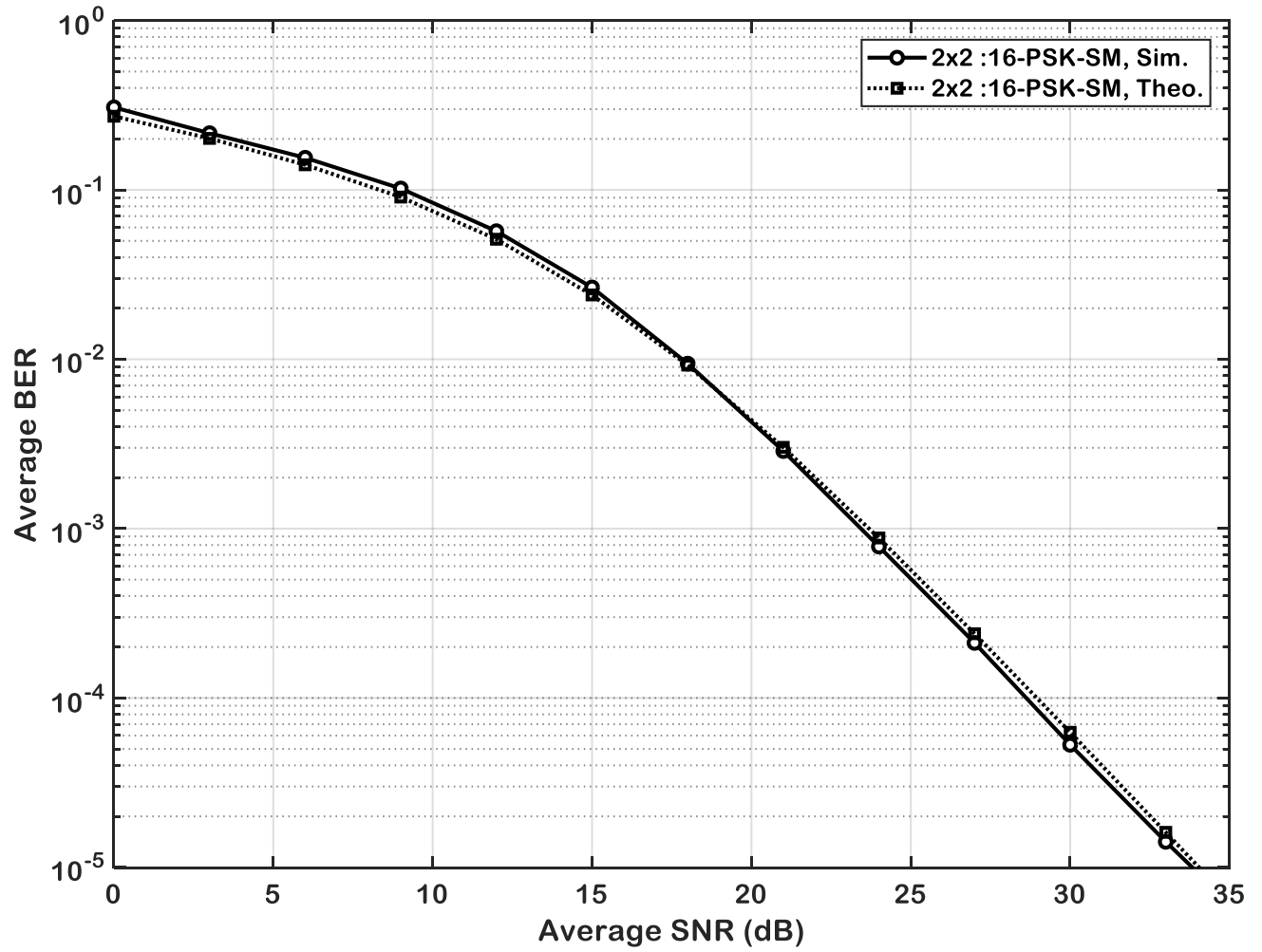


Figure 3-2: Monte Carlo simulation and Theoretical bounds for 16-PSK

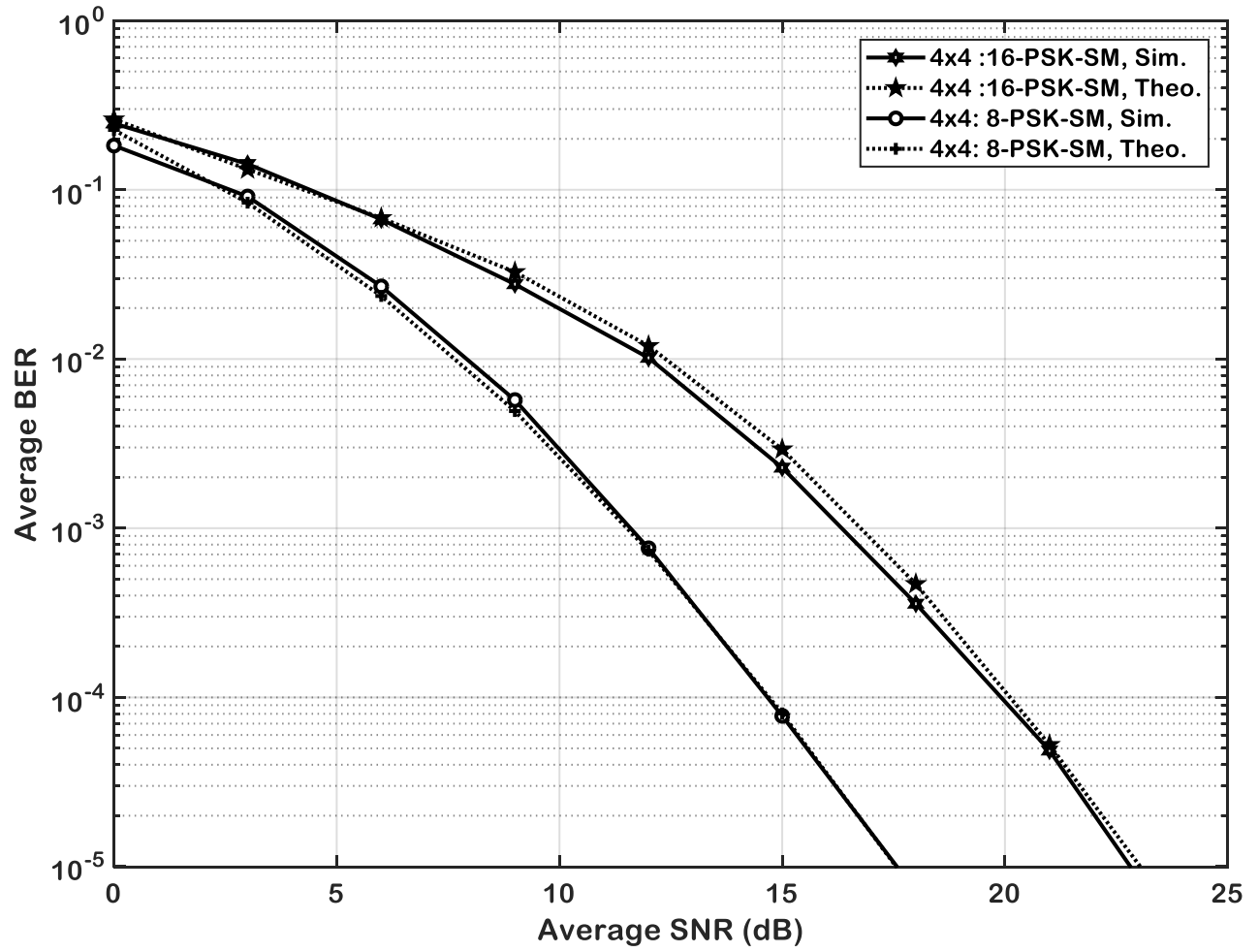


Figure 3-3: Monte Carlo simulation and Theoretical bounds for 16-PSK and 8-PSK

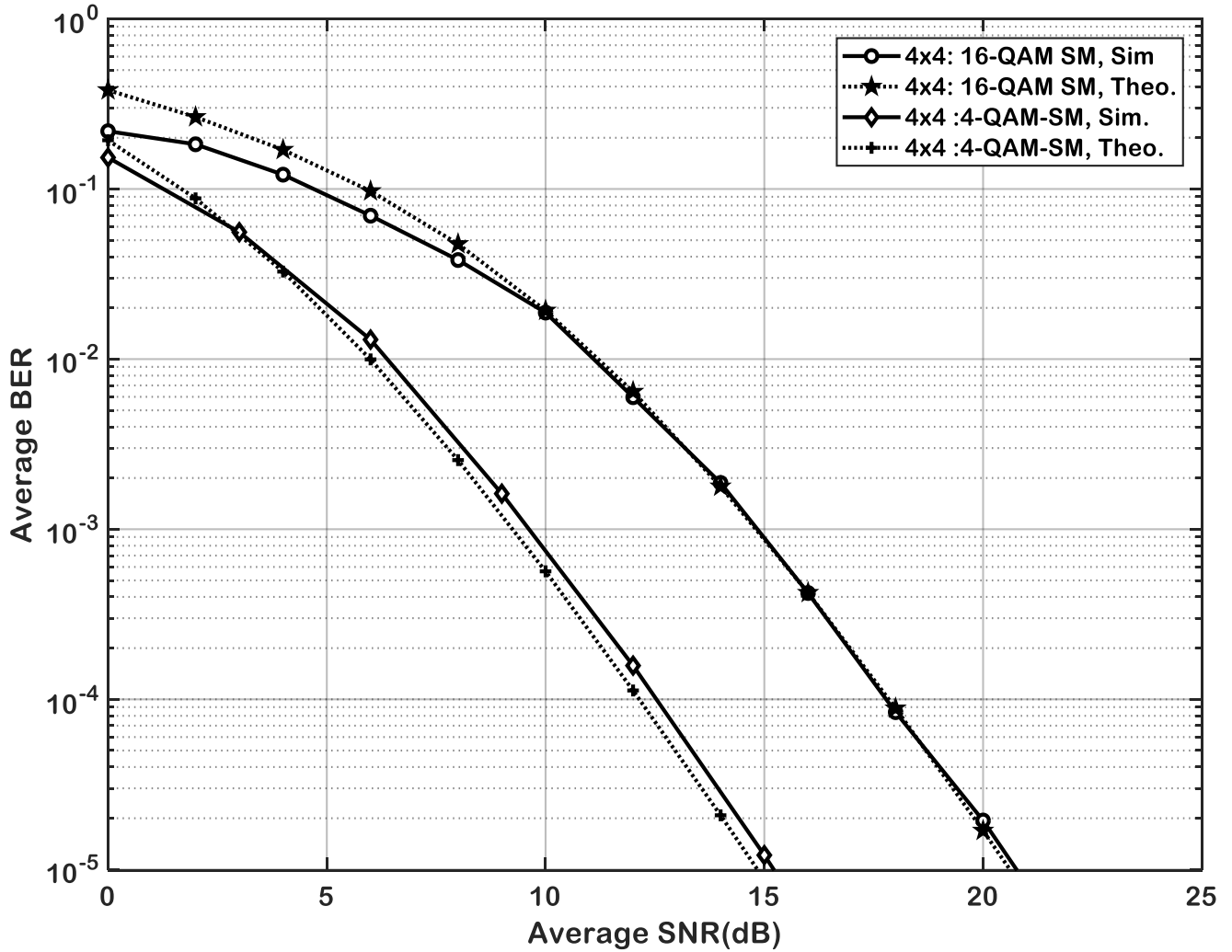


Figure 3-4: Monte Carlo simulation and Theoretical bounds for 4-QAM and 16-QAM

Validation of the analytical bounds presented in section 3.4 closely matched with Monte-Carlo simulation completed over i.i.d. Rayleigh fading channels as shown in Figure 3-2, Figure 3-3 and Figure 3-4. Maintaining the same antenna configuration and altering the size of the cardinality of the signal constellation diagram M , shows that increasing M degrades the error performance by 5 dB at BER value of 10^{-5} though the throughput is higher for the system with a higher M .

3.6 Chapter Synopsis

In this chapter, antenna diversity was presented in the form of Spatial Modulation. The outcome depicted a significant improvement in the error performance of a system with MIMO-SM configurations. Manipulating the size of the cardinality of the signal constellation diagram M and the antenna configuration while maintaining the throughput, showed an increase in performance for systems with high antenna configurations and low M . Thus, increasing the diversity subsequently increases the performance in SM. Finally, a theoretical closed-form lower bound was developed for MIMO-SM over i.i.d. Rayleigh fading channels which tightly matched with simulation results at high SNR

Chapter 4

Space-Time Block Coded Spatial Modulation

4.1. Introduction

The spatial multiplexing technique, SM, discussed in chapter 3 exhibits advantageous features such as totally avoiding ICI and IAS brought about the use of a single transmit antenna from a set of antennas where these remains dormant. Because of this reason, SM is more cost-effective and energy-efficient subsequently achieving high spectral efficiency. SM eliminates the limitations experienced by the conventional MIMO system and improves error performance.

The conventional SM scheme has some open issue such as; the number of transmit antennas has to be a power of two, and SM offers only a logarithmic increase in spectral efficiency with respect to the number of transmit antennas and does not achieve transmit diversity due to conveying information with a single transmit antenna at any given time. These impediments are remedied by the merging of SM and Alamouti STBC scheme termed Space-time block coded spatial modulation (STBC-SM) [6].

STBC-SM is a multiple-input-multiple-output (MIMO) technique based on the Alamouti scheme which exploits both advantages of space-time block codes and Spatial Modulation to improve the BER of SM through exploiting transmit diversity. The scheme uses two transmit antennas at any given time-slot. The pair of transmitted symbols are randomly selected from an MPSK/MQAM signal constellation. STBC-SM is presented in this thesis as a benchmark for the proposed scheme.

4.2. Transmission

Consider an $N_t \times N_r$ Alamouti STBC-SM scheme with c pairs of transmit antennas as per described in [6] where c is the total number of antenna combinations.

$$c = \left[\binom{N_t}{2} \right]_{2^p} \quad (4.1)$$

The number of transmitting and receiving antennas is denoted as N_t and N_r respectively. Figure 4-1 depicts the STBC-SM system model.

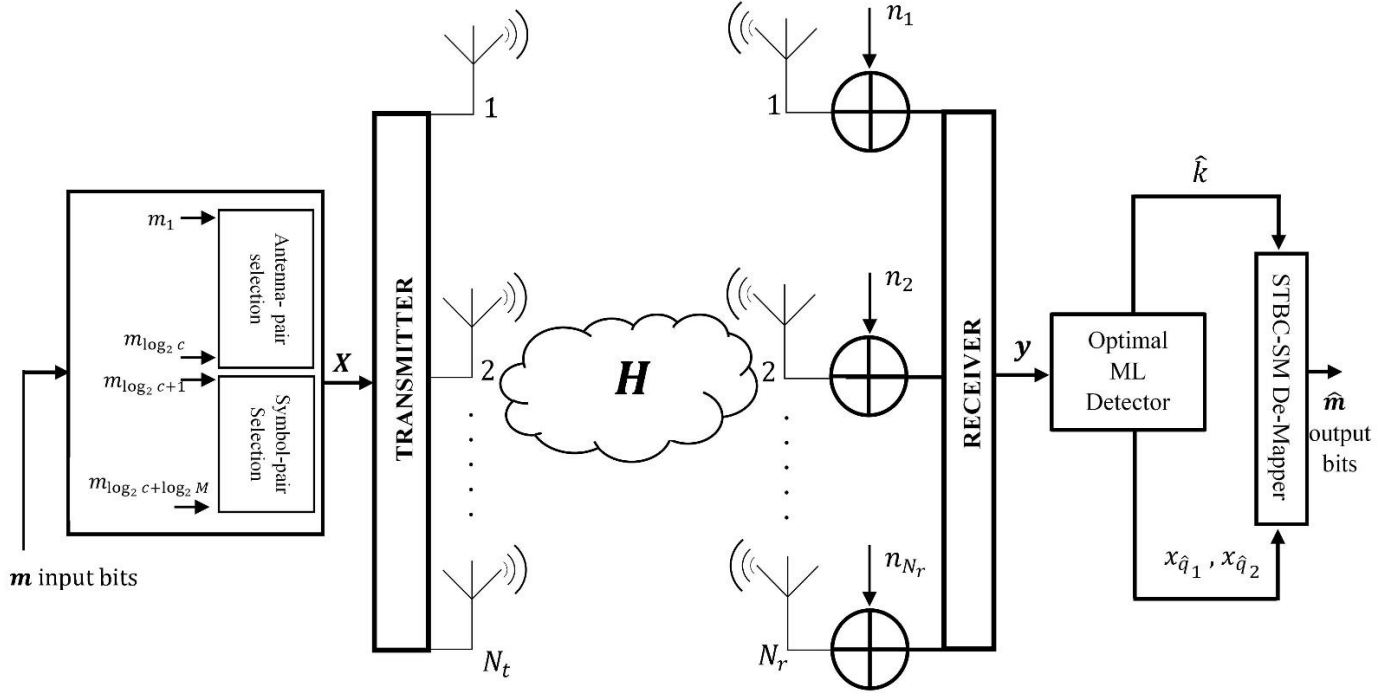


Figure 4-1: Alamouti STBC-SM system model [6]

The underlying aim behind STBC-SM scheme is to assign a vector of \mathbf{m} input bits stream of length $\log_2 c + 2\log_2 M$ to the STBC-SM mapper which will first map $\log_2 c$ bits to the k^{th} pair of transmit antennas k_1 and k_2 , such that the antenna combination k is expressed as $k = (k_1, k_2)$. The rest of the $2\log_2 M$ bits determine the M-PSK/M-QAM transmit symbol pairs, x_{q_1} , and x_{q_2} such that the spectral efficiency of the scheme is;

$$\eta_{STBC-SM} = \frac{1}{2} \log_2 c + \log_2 M \text{ bits/s/Hz} \quad (4.2)$$

The output from the signal mapping and spatial process can be expressed as [6]:

$$\begin{array}{ccccccc}
 & & k_1^{th} \text{ position} & & k_2^{th} \text{ position} & & \\
 & & \downarrow & & \downarrow & & \\
 \mathbf{X}_k = & \begin{pmatrix} 0 & \cdots & x_{q_1} & \cdots & x_{q_2} & \cdots & 0 \\ 0 & \cdots & -x_{q_2}^* & \cdots & x_{q_1}^* & \cdots & 0 \end{pmatrix}^T & & & & & \\
 & \uparrow & & & & & \uparrow & \\
 & 1^{st} \text{ position} & & & & & N_t^{th} \text{ position} &
 \end{array} \tag{4.3}$$

where $\mathbf{X}_k \in \chi$, $\chi = \{\mathbf{X}_k, k = 1, 2, \dots, c\}$ is the codeword with an $N_t \times 2$ dimension vector, x_{q_w} , $w \in [1: 2]$, resembles q_w^{th} symbols from an M-PSK/M-QAM constellation with $E[|x_{q_w}|^2] = 1$, and $x_{q_w} \in \Omega$, $\Omega = \{x_{q_w}, q_w = 1, 2, \dots, M\}$. q_w is the decimal index of the input information stream.

After the mapping process, the symbols are transmitted as per expression (4.4) where the columns represent the selected active transmit antenna-pair (k_1, k_2) . This is done over an $N_r \times N_t$ quasi-static Rayleigh fading channel $\mathbf{H} = [\mathbf{h}_1 \ \mathbf{h}_2 \ \cdots \ \mathbf{h}_{N_r}]$ where $\mathbf{h}_j = [h_{1,j} \ h_{2,j} \ \cdots \ h_{N_r,j}]^T$, $j \in [1: N_t]$ with an $N_r \times 2$ dimensional additive white Gaussian noise (AWGN) $\mathbf{N} = [n_1 \ n_2 \ \cdots \ n_{N_r}]^T$. The assumption is that both \mathbf{H} and \mathbf{N} entries have i.i.d. random variable according to $\mathbb{CN}(0,1)$ and $\mathbb{CN}(0,2/\rho)$ respectively and remains constant during two consecutive symbol intervals. At the receiver, the $N_r \times 2$ received signal vector \mathbf{Y} , over the two time-slots can be defined as

$$\mathbf{Y} = \mathbf{H}\mathbf{X}_k + \mathbf{N} \tag{4.4}$$

4.3. Detection

The conventional optimal Maximum Likelihood detector presented in [6] for the Alamouti STBC-SM scheme was employed at the receiver defined by expression (4.5). The assumption is that the detector has full knowledge of the channel at the receiver. The optimal ML performs a combined estimation of the transmitted symbol pair index and transmit antenna pair index, thus totally exploiting the advantages of

Alamouti STBC-SM. A comprehensive search over all possible cM^2 unique transmission matrices is done and the matrix which minimizes (4.5) is chosen.

$$\hat{\mathbf{X}}_k = \underset{\mathbf{X}_k \in \mathcal{X}}{\operatorname{argmin}} \|\mathbf{Y} - \mathbf{H}\mathbf{X}_k\|_F^2 \quad (4.5)$$

4.4. Performance Analysis

The derivation of an asymptotic performance bound for the average BER of M-PSK/M-QAM Alamouti STBC-SM in i.i.d. Rayleigh flat fading channel conditions is presented in this section. Xu *et al.* [31] presented a tight closed-form bound for a square M-QAM Alamouti STBC-SM over i.i.d. Rayleigh frequency-flat fading channel. He demonstrated that Alamouti STBC system with two transmit antennas and arbitrary receive antennas are tantamount to MRC system having one transmit antenna and $2N_r$ receive antennas with a 3 dB loss [6]. Therefore, an $N_t \times N_r$ STBC-SM with c pair of transmit antennas can be regarded as a $c \times 2N_r$ SM system with 3 dB loss [31].

In section 4.3, the detector approximations the transmitted symbol indices and the antenna pair index making the BER dependent on two estimation processes. Xu *et al* [31], assumes that the two estimation processes are independent of each other, thus the overall BER is given by (4.6), where P_a resembles the BEP of estimating the antenna pair index assuming that the symbols are correctly detected and P_d resembles the BEP of estimating symbols assuming that the transmit antenna pairs are correctly detected. The BEP of estimating the antenna pair index is halved that of SM system due to the use of two time-slots to convey the antenna information as reasoned by Xu *et al* [31], hence the overall BEP is given as:

$$P_e \geq \frac{P_a}{2} + P_d - \left(\frac{P_a}{2}\right)P_d \quad (4.6)$$

where P_a for an $N_t \times N_r$ systems with c transmit antenna pairs is given by [31]:

$$P_a \leq \sum_{k=1}^c \sum_{\hat{k}=1}^c \sum_{q=1}^M \frac{N(k, \hat{k}) \mu_\alpha^{2N_r} \sum_{w=0}^{2N_r-1} \binom{2N_r-1+w}{w} [1-\mu_\alpha]^w}{cM} \quad (4.7)$$

where $N(k, \hat{k})$ is the number of bits in error between transmitted transmit antenna index k and estimated phase index \hat{k} , $\mu_\alpha = \frac{1}{2} \left(1 - \sqrt{\frac{\sigma_\alpha^2}{1+\sigma_\alpha^2}} \right)$, $\sigma_\alpha^2 = \left(\frac{\rho}{2} \right) |x_q|^2$, $q \in [1 : M]$.

P_d , the BEP of either PSK/QAM symbols is expressed below.

$$P_{d_{QAM}} = \frac{a}{mn} \left\{ \frac{1}{2} \left(\frac{2}{b\rho+1} \right)^{2N_r} - \frac{a}{2} \left(\frac{1}{b\rho+1} \right)^{2N_r} + (1-a) \sum_{k=1}^{n-1} \left(\frac{S_k}{b\rho+S_k} \right)^{2N_r} + \sum_{k=1}^{2n-1} \left(\frac{S_k}{b\rho+S_k} \right)^{2N_r} \right\} \quad (4.8)$$

where $a = \left(1 - \frac{1}{\sqrt{M}} \right)$, $b = \frac{3}{M-1}$, $m = \log_2 M$, n is the number of iterations for convergence and $S_k = 2 \sin^2 \left(\frac{k\pi}{4n} \right)$

$$P_{d_{PSK}} = \frac{M-1}{Mmn} \left[\frac{1}{2} \left(\frac{\sin^2 \theta}{\sin^2 \theta + \rho \sin^2 \beta} \right)^{2N_r} + \sum_{k=1}^{n-1} \left(\frac{\sin^2 \frac{k\theta}{n}}{\sin^2 \frac{k\theta}{n} + \rho \sin^2 \beta} \right)^{2N_r} \right] \quad (4.9)$$

where $\theta = \pi - \beta$, $\beta = \pi/M$, $m = \log_2 M$, M is the symbol constellation size, ρ is the scaled average SNR at each receive antenna and n is the number of iterations greater than 10.

4.5. Analytical and Simulation Results

This section presents the analytical framework and simulations results of MPSK-SM and MPSK STBC-SM with the following antenna configurations:

- i. 4×4 : 8-PSK STBC SM and 4×4 : 8-PSK SM
- ii. 4×4 : 16-PSK STBC SM and 4×4 : 16-PSK SM
- iii. 4×4 : 8-QAM STBC SM, 4×4 : 4-QAM SM and 2×2 : 16-QAM Alamouti STBC

Monte Carlo simulations performed over i.i.d. Rayleigh flat fading channels were validated with the analytical framework presented in Section 2.2. Comparisons are drawn at BER value of 10^{-5} with the assumption that: full knowledge of the channel is available at the receiver; the transmit and receive antennas are spaced to avoid correlation.

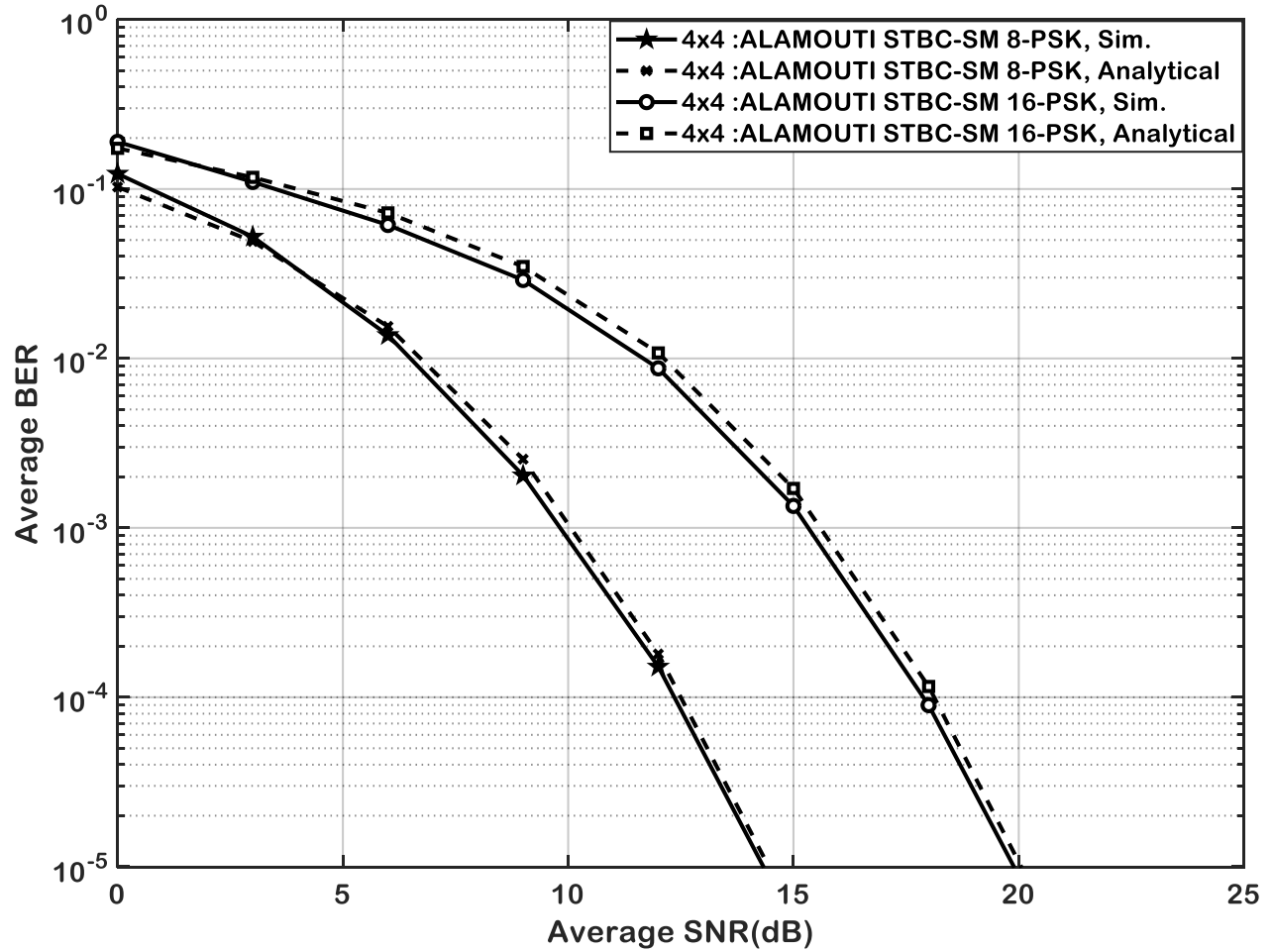


Figure 4-2: Monte Carlo simulation and Theoretical bounds for 8-PSK STBC-SM and 16-PSK STBC-SM

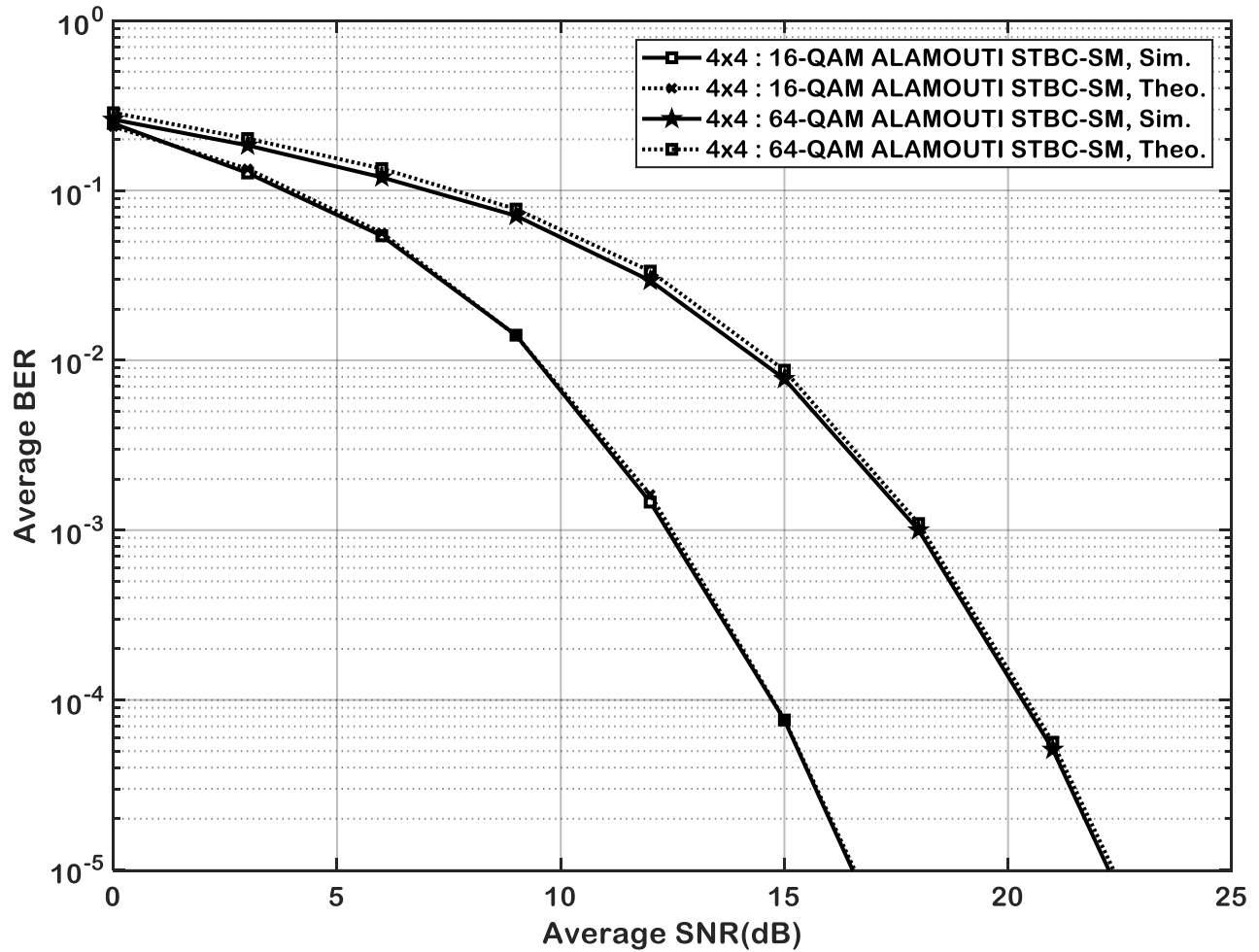


Figure 4-3: Monte Carlo simulation and Theoretical bounds for 16-QAM STBC-SM and 64-QAM STBC-SM

The analytical bound matched with Monte-Carlo simulations performed over i.i.d. Rayleigh flat fading channel as presented in Figure 4-2 and Figure 4-3 validating the framework developed in section 2.2. Increasing the size of the cardinality of the signal constellation diagram M from 8 to 16 while keeping the antenna configurations, degrades the performance of the system by 5.6 dB in Figure 4-2 whereas Figure 4-3 shows the degradation of square QAM with M form 16 to 64 of 5.8 dB at a BER of 10^{-5} while increasing the spectral efficiency by 1b/s/Hz and 2 b/s/Hz respectively.

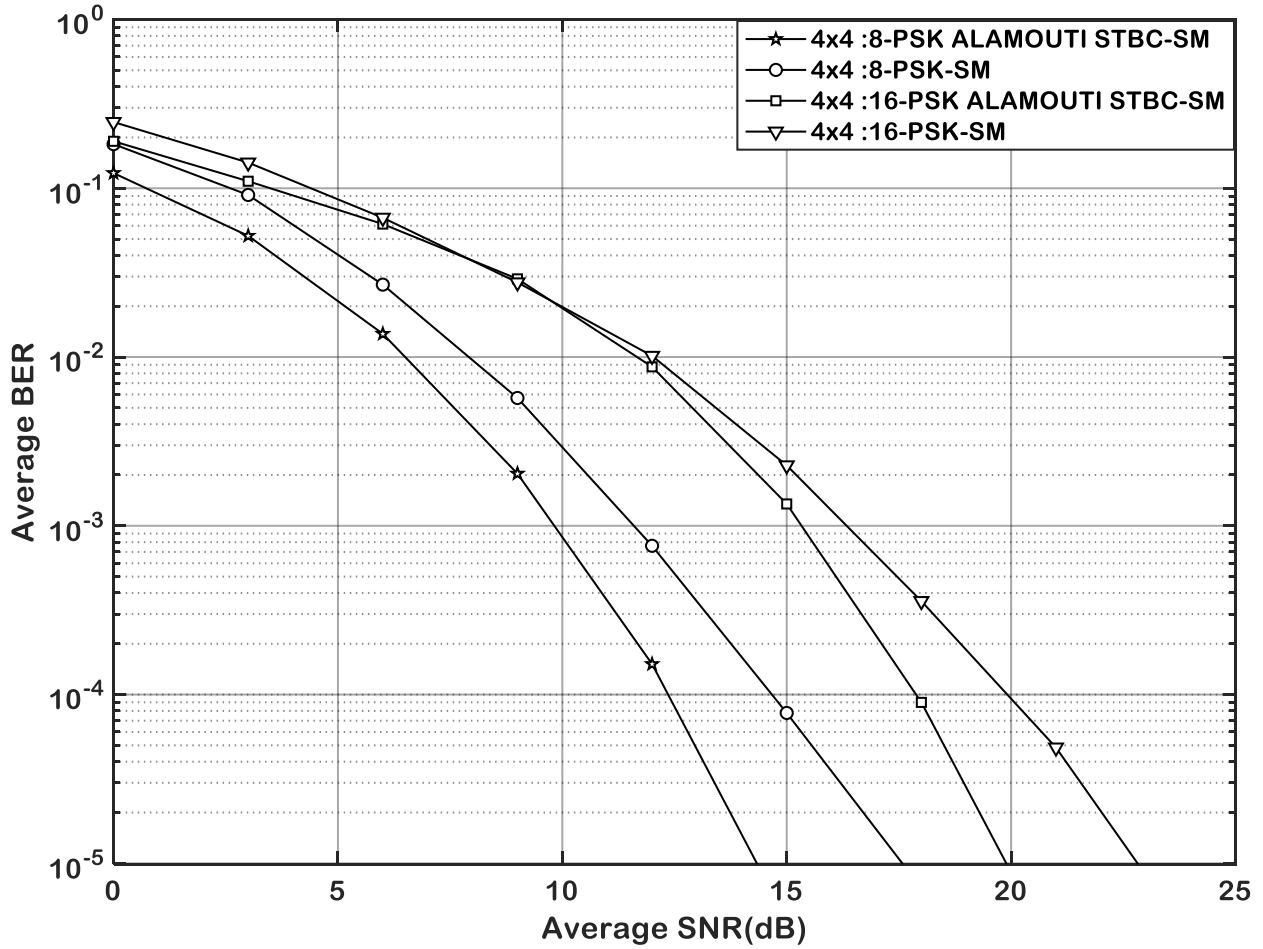


Figure 4-4: BER performance of 8/16-PSK STBC-SM and 8/16-PSK SM

Again, keeping the antenna configurations of SM and Alamouti STBC-SM at parity and increasing the size of the cardinality of the constellation diagram M for both schemes and comparing them at the parity state, the latter scheme has a gain of 3.2 dB and 3 dB for $M = 8$ and $M = 16$ respectively. It is apparent from Figure 4-4 that Alamouti STBC aids the performance of SM through the introduction of spatial diversity.

4.6. Chapter Synopsis

Evidently, from Figure 4-4, the Alamouti STBC-SM scheme offers a substantial improvement in error performance when matched to the conventional SM through exploiting transmit diversity. For example; for 8-PSK and 16-PSK schemes having a 4×4 configuration, Alamouti STBC-SM outclasses the conventional SM by approximately 3.2 dB and 3 dB respectively at a BER of 10^{-5} though coming at the expense of an acceptable linear increase in decoding complexity. Furthermore, it has been revealed that STBC-SM improves the BER performance compared to SM. The analytical bound of STBC-SM was validated with Monte-Carlo simulations performed over i.i.d. Rayleigh flat fading channel which showed a tight match.

Chapter 5

Enhanced Spectral Efficiency of Alamouti Space-time block coded Spatial Modulation Using Unitary Matrix Transformation (E-STBC-SM)

5.1. Introduction

The ingenious exploitation and merging of both spatial multiplexing scheme and spatial diversity scheme i.e. SM and Alamouti STBC gave birth to a robust, high rate and low complexity scheme called STBC-SM. A concerted effort by researchers to further enhance the data rate of the scheme has been made due to its usefulness for low complexity and emerging wireless communication systems [6].

To further enhance the spectral efficiency, a high rate STBC-SM (H-STBC-SM) scheme and a spatial modulation STBC with Cyclic structure were introduced [41, 42]. Both schemes deliver twice the codewords provided by the conventional STBC-SM scheme and the diversity order of both schemes is two. Nonetheless, H-STBC-SM undergoes a slight loss in error performance. Furthermore, at the same spectral efficiency and with fewer transmit antennas needed than the conventional STBC-SM, STBC-CSM's performance approaches that of STBC-SM.

Another form of high-rate space-time block coded spatial modulation (HR-STBC-SM) was proposed in [43] where the transmission matrix is nothing but a simple linear combination of two Alamouti scheme. The HR-STBC-SM scheme increases the data rate and achieves a transmit diversity of the order two. In contrast with the conventional Alamouti STBC, the HR-STBC-SM transmits two symbols over one-time slot, thus its rate is two symbols per channel use (pcu) compared to the one symbol pcu provided by the former.

An alternative method to enhance the data rate while keeping the principles of the conventional Alamouti STBC-SM, is by applying the unitary transformation to space-time blocks where the cardinality of the space-time block is increased [44]. Unitary matrix transformation improves spectral efficiency by expanding the space-time code. The Conventional Alamouti STBC scheme is expanded using the unitary matrix transformation thereby improving the throughput.

5.2. The STBC Expansion

Unitary matrix transformation is the multiplication of the conventional transmission matrix of space-time codes by unitary matrices [12]. Unitary matrices are an $M \times M$ matrices with only diagonal non-zero entries. Multiplying the conventional Alamouti STBC transmission matrix with the aforementioned matrices expands STBC and also introduces redundancy. Of note, unitary matrix transformation does not increase the size of the resulting APM symbol set, hence preventing an increase in the PAPR (peak-to-average power ratio) of the transmitted symbol [12]. In order to send d extra bits per space-time codeword, a sum of 2^d diagonal unitary matrices is needed. The employed diagonal matrices are of the form shown in (5.1).

$$\mathbf{U} = \begin{bmatrix} e^{j\theta_1} & 0 \\ 0 & e^{j\theta_2} \end{bmatrix} \quad 0 \leq \theta_i < 2\pi, i \in [1:2] \quad (5.1)$$

where θ_1 and θ_2 are mutable rotational angles. To find the 2^d combinations of θ_1 and θ_2 , which gives a set of unitary matrices having an optimal Euclidean distance distribution, a computer-aided numerical search can be utilized [12]. The optimal Euclidean distribution is achievable by keeping θ_1 constant at zero while varying θ_2 in equal intervals over the range of 2π [12], [45]. The unitary matrices shown in (5.2) for STBC expansion are employed in this dissertation which is consistent with the above discussion. The proposed scheme will thus be termed as enhanced spectral efficiency of Alamouti space-time block coded spatial modulation (E-STBC-SM).

$$\mathbf{U}_\ell = \begin{bmatrix} 1 & 0 \\ 0 & e^{j\theta_\ell} \end{bmatrix} \quad \ell \in \mathbb{Z}_{\geq 0} \quad (5.2)$$

where the angle of rotation is defined as $\theta_\ell = \frac{2\pi}{2^d} \ell$ for all $\ell \in [0 : 2^d - 1]$, \mathbb{Z} is the set of positive integers. High rate STBC's is the product of the transpose of Alamouti STBC transmission matrix \mathbf{X} (2.1) and (5.2) expressed as

$$\mathbf{X}_k = \mathbf{X}\mathbf{U}_\ell \quad (5.3)$$

In expanded form, the high rate STBC is given as

$$\mathbf{X}_k = \begin{bmatrix} x_1 & x_2 e^{j\theta_\ell} \\ -x_2^* & x_1^* e^{j\theta_\ell} \end{bmatrix} \quad (5.4)$$

where θ_ℓ encodes the additional bits. They are M^2 possible combinations of symbols x_1 and x_2 where M is the order of modulation. Table (5-1) below shows the additional bits corresponding to the rotational angle θ_ℓ with equal intervals over the range of 2π .

Table 5-1: Additional bits with corresponding rotational angles

Additional Bits	Rotational Angles intervals
$b_1 = 1$	$\theta_1 = \pi$
$b_2 = 2$	$\theta_1 = \frac{\pi}{2}$
$b_3 = 3$	$\theta_1 = \frac{\pi}{4}$
$b_4 = 4$	$\theta_1 = \frac{\pi}{8}$
$b_5 = 5$	$\theta_1 = \frac{\pi}{16}$

5.3. Transmission

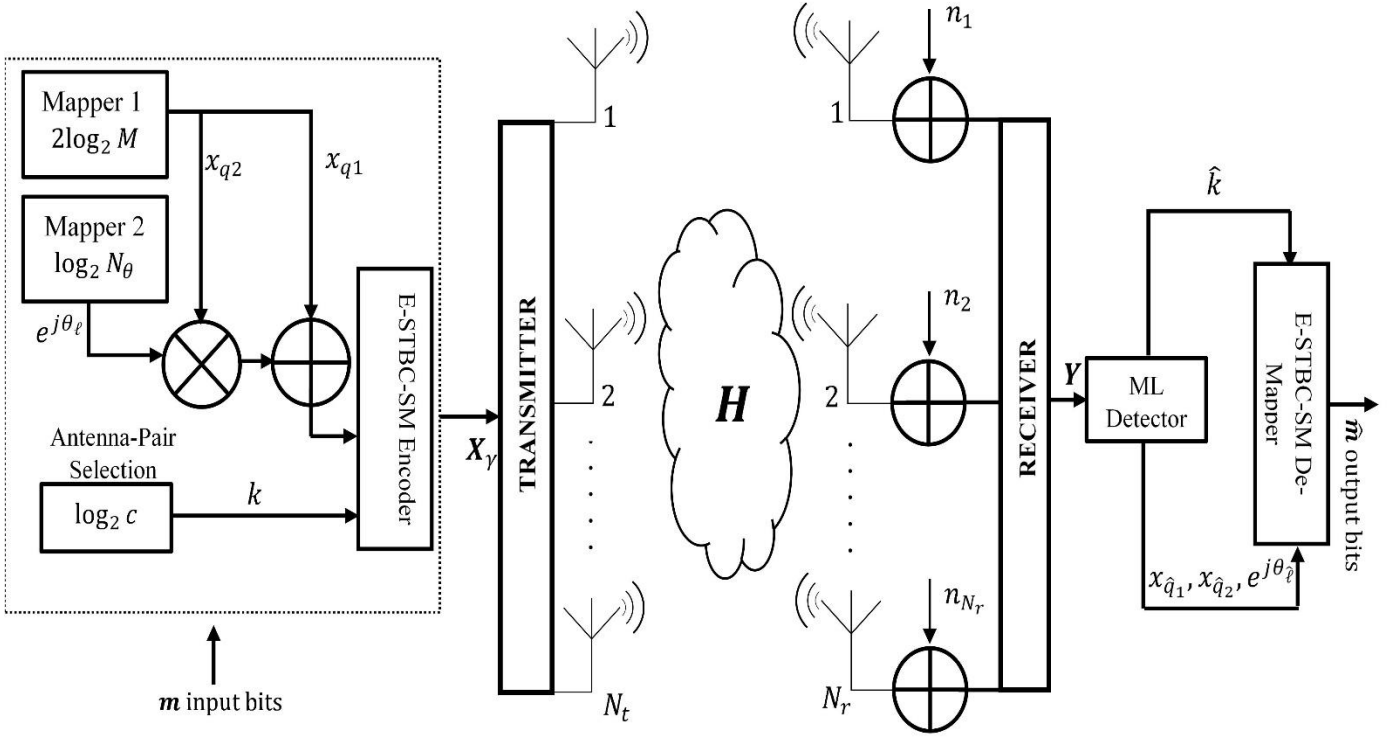


Figure 5-1: E-STBC-SM system model

Consider an $N_t \times N_r$ Alamouti E-STBC-SM system with

$$c = \left[\binom{N_t}{N_u} \right]_{2^p} \quad (5.5)$$

pairs of transmit antennas as per described in [7] where c is the overall number of transmit antenna combinations (TAC). The number of transmit and receive antennas is denoted as N_t and N_r respectively. N_u denotes the number of active antennas at any particular time-slot. However, the TAC must be a power of two, therefore, the total legitimate pairs are given by $N = 2^{\log_2 c}$ and the of the pairs are discarded [45]. The legitimate TAC's are the optimal set designated by exploiting the knowledge of the CSI based on maximizing the minimum Euclidean distance [46], hence optimal TAC set for $N_t = 4, N_u = 2$ is $N = [(1,3) (1,4) (2,3) (2,4)]$.

The objective behind the E-STBC-SM is to assign a vector \mathbf{m} with an input bits stream to the E-STBC-SM mapper which will constitute $\log_2 c$ bits to the k^{th} pair of transmit antennas k_1 and k_2 , $\log_2 N_\theta$ bits to the phase component θ_ℓ which determines the size of the constellation mapping for the additional bits corresponding to a PSK mapper and finally $2\log_2 M$ bits to the M-PSK/M-QAM symbols x_{q_1} and x_{q_2} such that the total transmitted bits of the scheme is given by $\mathbf{m} = \log_2 c + \log_2 N_\theta + 2\log_2 M$ and the Spectral efficiency is

$$\eta_{E-STBC-SM} = \frac{1}{2}\log_2 c + \frac{1}{2}\log_2 N_\theta + \log_2 M \quad (5.6)$$

The output of the signal mapping and spatial process can be expressed as:

$$\mathbf{X}_\gamma = \begin{pmatrix} 0 & \cdots & \overset{k_1^{th} \text{ position}}{\downarrow} x_{q_1} & \cdots & \overset{k_2^{th} \text{ position}}{\downarrow} x_{q_2} e^{j\theta_\ell} & \cdots & 0 \\ 0 & \cdots & -x_{q_2}^* & \cdots & x_{q_1}^* e^{j\theta_\ell} & \cdots & 0 \end{pmatrix}^T \quad (5.7)$$

\uparrow 1^{st} position \uparrow $N_t^{th} \text{ position}$

where $\mathbf{X}_\gamma \in \mathcal{X}, \mathcal{X} = \{\mathbf{X}_\gamma, \gamma \in [1:c]\}$ is the codeword matrix with an $N_t \times 2$ dimension vector specifying the initiated antenna pair during which all the other antennas remain idle, $x_{q_w}, w \in [1:2]$, resembles q_w^{th} symbols from a PSK/QAM constellation with $E[|x_{q_w}|^2] = 1$, and $x_{q_w} \in \zeta, \zeta = \{x_{q_w}, q_w = 1, 2, \dots, M\}$.

The phase component, $e^{j\theta_\ell}$, subsequently translates to a PSK symbol set which can have constellation sizes $N_\theta = 2^d$ where $d \geq 1$ is the number of additional bits required. This symbol set which also has unit average power is purely for rotating the x_{q_2} symbol during transmission.

After the mapping process, the symbols are transmitted as per expression (5.8) where the columns represent the selected active antenna-pair (k_1, k_2) . This is done over an $N_r \times N_t$ quasi-static Rayleigh fading channel which lasts for two time slots $\mathbf{H} = [\mathbf{h}_1 \quad \mathbf{h}_2 \quad \cdots \quad \mathbf{h}_{N_t}]$ where $\mathbf{h}_j = [h_{1,j} \quad h_{2,j} \quad \cdots \quad h_{N_r,j}]^T, j \in [1: N_t]$ with $N_r \times 2$ dimensional additive white Gaussian noise (AWGN) $\mathbf{N} = [n_1 \quad n_2 \quad \cdots \quad n_{N_r}]^T$. The assumption is that both \mathbf{H} and \mathbf{N} have i.i.d. random variable according to $\mathbb{CN}(0,1)$ and $\mathbb{CN}(0,2/\rho)$ distribution respectively which remains constant during a consecutive pair of time slots. At the receiver, the $N_r \times 2$ received signal vector \mathbf{Y} , over the two-time slots can be defined as

$$\mathbf{Y} = \mathbf{H}\mathbf{X}_\gamma + \mathbf{N} \quad (5.8)$$

In addition, E-STBC-SM scheme exploits the orthogonality of Alamouti STBC [6].

5.4. Detection

The Detection is done with the use of an ML detector. The detector is assumed to have full knowledge of the channel at the receiver. The ML fully exploits the advantages of Alamouti STBC-SM by carrying out a combined detection of the active transmit antenna pair index, the modulated phase symbol index as well as the modulated symbols pair index. This is done by the decoder performing a comprehensive search through all possible $cN_\theta M^2$ unique transmission matrices and chooses the matrix which minimizes equation (5.9) below.

$$\hat{\mathbf{X}}_\gamma = \underset{\mathbf{X}_\gamma \in \mathcal{X}}{\operatorname{argmin}} \|\mathbf{Y} - \mathbf{H}\mathbf{X}_\gamma\|_F^2 \quad (5.9)$$

5.5. Theoretical Analysis of E-STBC-SM

The analytical bound for M -ary M-PSK STBC-SM over i.i.d. Rayleigh flat fading channel conditions are derived. Applying the method in [14], the transmitted symbol pair and transmit antenna pair index approximation processes are considered to be independent. On this basis, the union bound of the average BER for the proposed scheme has been derived. Let P_θ denote BEP of estimating the phase given that the pair of transmit antennas and symbols are correctly detected and P_d denotes BEP of estimating the symbols assuming that the phase is correctly detected. The overall probability of bit-error is then bounded by

$$P_e \geq P_\theta + P_d - P_\theta P_d \quad (5.10)$$

5.5.1. Analytical BER for Estimated Symbol Pair

The union bound technique encapsulated in [17] is applied to derive the BER of the symbol pair estimation. Assuming that the phase ($e^{j\theta_\ell}$) is detected without error and \mathbf{H} is known at the receiver, the equivalent model of the system is found to be:

$$Z_1 = \left(\|\mathbf{h}_1\|^2 + \|\tilde{\mathbf{h}}_2\|^2 \right) x_1 + \tilde{n}_1$$

$$Z_2 = \left(\|\mathbf{h}_1\|^2 + \|\tilde{\mathbf{h}}_2\|^2 \right) x_2 + \tilde{n}_2$$

where $\tilde{\mathbf{h}}_2 = e^{j\theta_\ell} \mathbf{h}_2$ showing that the performance is analogous to the Alamouti scheme having a 3 dB attenuation compared to MRC. In accordance to work in section 2.5 of chapter 2, the BEP of the estimated symbol pair is then bounded by expressions (2.9) and (2.10) with respect to the modulation scheme.

5.5.2. Analytical BER for the Phase Symbol

The following subsection details the theoretical ABEP of the additional bits employing the union bound technique. In accordance with the assumption that at high SNR the transmitted symbol pair is correctly detected while the phase symbol is detected with error, the average BEP of the phase estimation is defined by:

$$P_\theta \geq \sum_{\ell=1}^{N_\theta} \sum_{\hat{\ell}=1}^{N_\theta} \frac{N(\ell, \hat{\ell}) P(e^{j\theta_\ell} \rightarrow e^{j\theta_{\hat{\ell}}})}{\log_2 N_\theta} \quad (5.12)$$

where $P(e^{j\theta_\ell} \rightarrow e^{j\theta_{\hat{\ell}}})$ is the pairwise error probability (PEP) of choosing the phase vector $e^{j\theta_{\hat{\ell}}}$ given that $e^{j\theta_\ell}$ was transmitted and $N(\ell, \hat{\ell})$ is the number of bits in error between transmitted phase index ℓ and estimated phase index $\hat{\ell}$, N_θ is the number of bits transmitted by $e^{j\theta_\ell}$. Assuming that x_1 and x_2 are detected correctly and are known at the receiver, the received signal can be written as follows;

$$\begin{aligned} \mathbf{y}_1 &= e^{j\theta_\ell} \mathbf{h}_2 x_2 + \mathbf{n}_1 \\ \mathbf{y}_2 &= e^{j\theta_\ell} \mathbf{h}_2 x_1^* + \mathbf{n}_2 \end{aligned} \quad (5.13)$$

Hence, the BEP of the phase symbol is derived. The PEP $P(e^{j\theta_\ell} \rightarrow e^{j\theta_{\hat{\ell}}})$ of choosing signal ($e^{j\theta_{\hat{\ell}}}$) given that ($e^{j\theta_\ell}$) was transmitted is given by

$$P(e^{j\theta_\ell} \rightarrow e^{j\theta_{\hat{\ell}}}|x_1, x_2, \mathbf{h}_2) = P \left(\begin{aligned} &\|\mathbf{y}_1 - e^{j\theta_\ell} \mathbf{h}_2 x_2\|_F^2 + \|\mathbf{y}_2 + e^{j\theta_\ell} \mathbf{h}_2 x_1^*\|_F^2 \\ &> \|\mathbf{y}_1 - e^{j\theta_{\hat{\ell}}} \mathbf{h}_2 x_2\|_F^2 + \|\mathbf{y}_2 + e^{j\theta_{\hat{\ell}}} \mathbf{h}_2 x_1^*\|_F^2 \end{aligned} \right) \quad (5.14)$$

After substitution, (5.14) Reduces to (See Appendix A for complete derivation);

$$P(e^{j\theta_\ell} \rightarrow e^{j\theta_{\hat{\ell}}}|x_1, x_2, \mathbf{h}_2) = Q\left(\sqrt{\frac{\rho d_2}{2}}\right) \quad (5.15)$$

where ρ is the average SNR at each receive antenna, $d_2 = |e^{j\theta_\ell} \rightarrow e^{j\theta_{\hat{\ell}}}|^2$ and $Q(\delta)$ is the Gaussian Q-function.

With further simplification, we arrive at

$$P(e^{j\theta_\ell} \rightarrow e^{j\theta_{\hat{\ell}}}) = \frac{1}{2n} \left[\frac{1}{2} \left(\frac{2}{2 + \rho d_2} \right)^{N_r} + \sum_{k=1}^{n-1} \left(\frac{2 \sin^2 \theta}{2 \sin^2 \theta + \rho d_2} \right)^{N_r} \right] \quad (5.16)$$

The average BER performance can then be obtained by back substituting equation (5.16) into (5.12). n is the number of iterations for convergence ($n > 10$) [47]. The overall probability of bit-error P_e is then obtained as per expression (5.10).

5.6. Analytical and Simulation results

The following section presents the analytical framework and simulation results of E-STBC-SM for the listed antenna configurations:

- i. 4×4 : 16-PSK STBC SM and 4×4 : 16-PSK E-STBC SM
- ii. 4×4 : 16-PSK STBC SM and 4×4 : 16-PSK E-STBC SM $\left(\theta \in \left[\frac{\pi}{2}, \frac{\pi}{4}\right]\right)$
- iii. 4×4 : 32-PSK STBC SM and 4×4 : 32-PSK E-STBC SM $\left(\theta \in \left[\frac{\pi}{2}, \frac{\pi}{4}, \frac{\pi}{8}\right]\right)$
- iv. 4×4 : 64-PSK STBC SM and 4×4 : 64-PSK E-STBC SM $\left(\theta \in \left[\frac{\pi}{2}, \frac{\pi}{4}, \frac{\pi}{8}, \frac{\pi}{16}\right]\right)$
- v. 4×4 : 64-QAM STBC SM and 4×4 : 64-QAM E-STBC SM $\left(\theta \in \left[\frac{\pi}{8}, \frac{\pi}{16}\right]\right)$

Monte Carlo simulations carried out over i.i.d. Rayleigh flat-fading channel is validated with the analytical framework presented in Section 5.5. Evaluations were made at BER value of 10^{-5} with the assumption that full knowledge of the channel is available at the receiver, the transmit and receive antennas are spaced to avoid correlation.

At high SNR regions, the theoretical bound is witnessed to closely estimated the average BER performance. In a comparison of the two schemes, the performance is the same even though the proposed E-STBC-SM has an improvement Spectral efficiency of an additional two information bits.

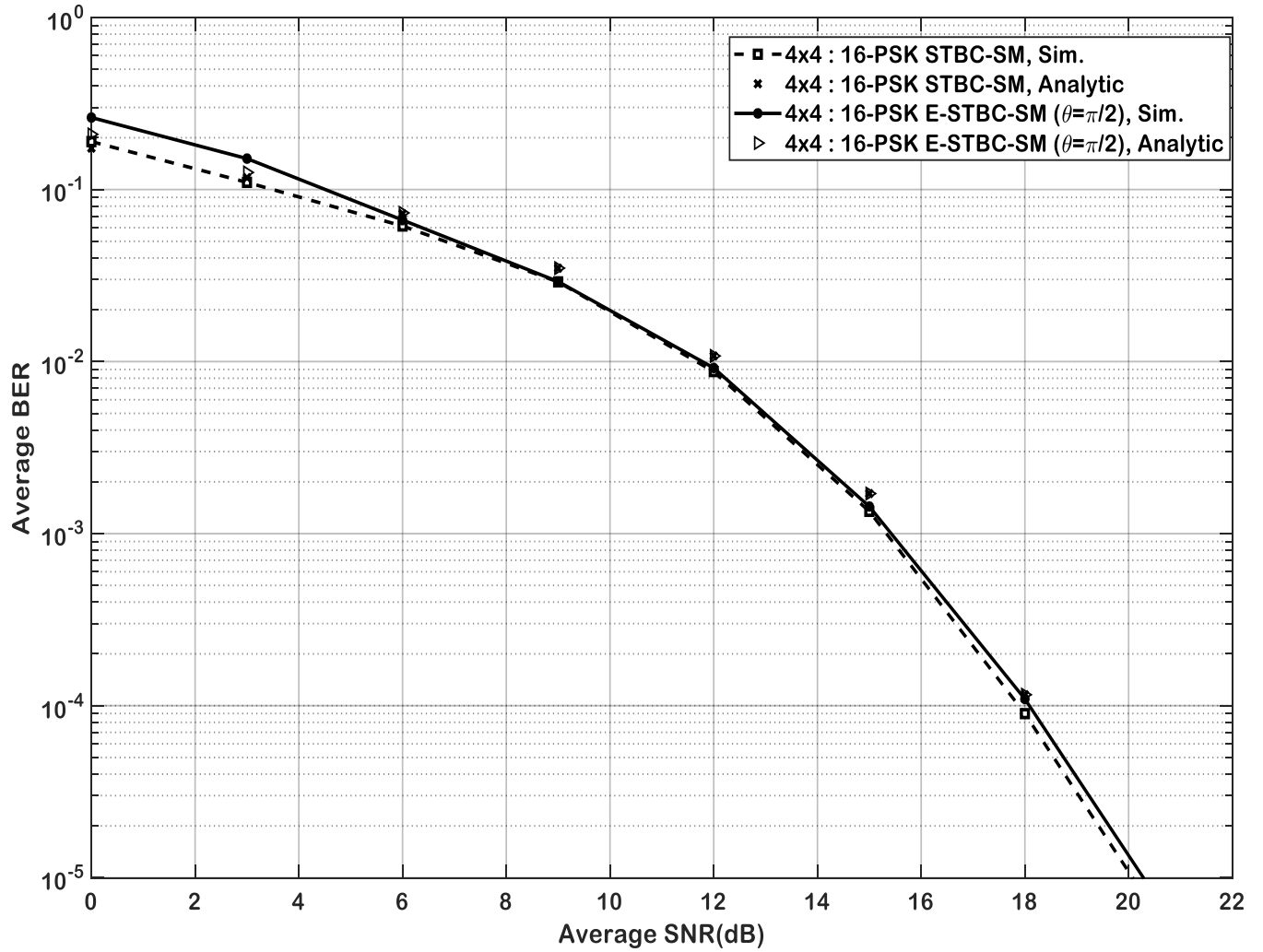


Figure 5-2: Theoretical and Simulated Average BER

The following four figures show that with additional bits brought about by altering the rotational angle θ_ℓ , the E-STBC-SM system increases the throughput while maintaining similar diversity of STBC-SM though with minimal degradation in performance.

Firstly, Figure 5-3 depicts the results of an M-PSK STBC-SM scheme against the proposed M-PSK E-STBC-SM scheme where $M = 16$ with the former having a throughput of 10 b/s/Hz. The expansion, as per the discussion in section 3.1 with a maximum of $\theta = \frac{\pi}{4}$, gives an additional 3 bits to the STBC-SM scheme. Using expressions (4.9) and (5.6), the spectral efficiency increases from 5 b/s/Hz to a maximum of 6.5 b/s/Hz respectively. An attenuation in error performance of 0.6 dB is experienced as a result of the expansion.

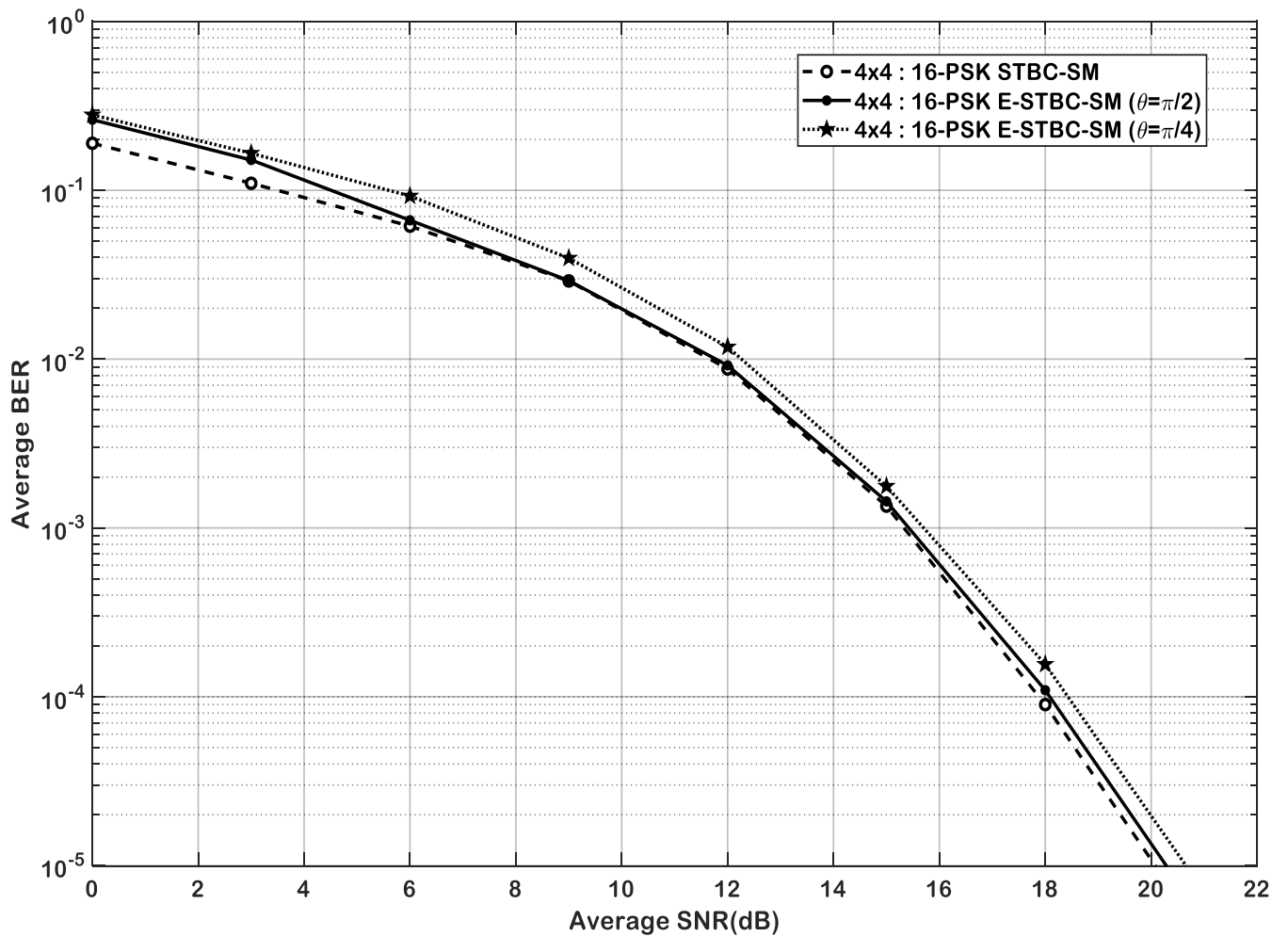


Figure 5-3: BER performance of 16-PSK STBC-SM and 16-PSK E-STBC-SM

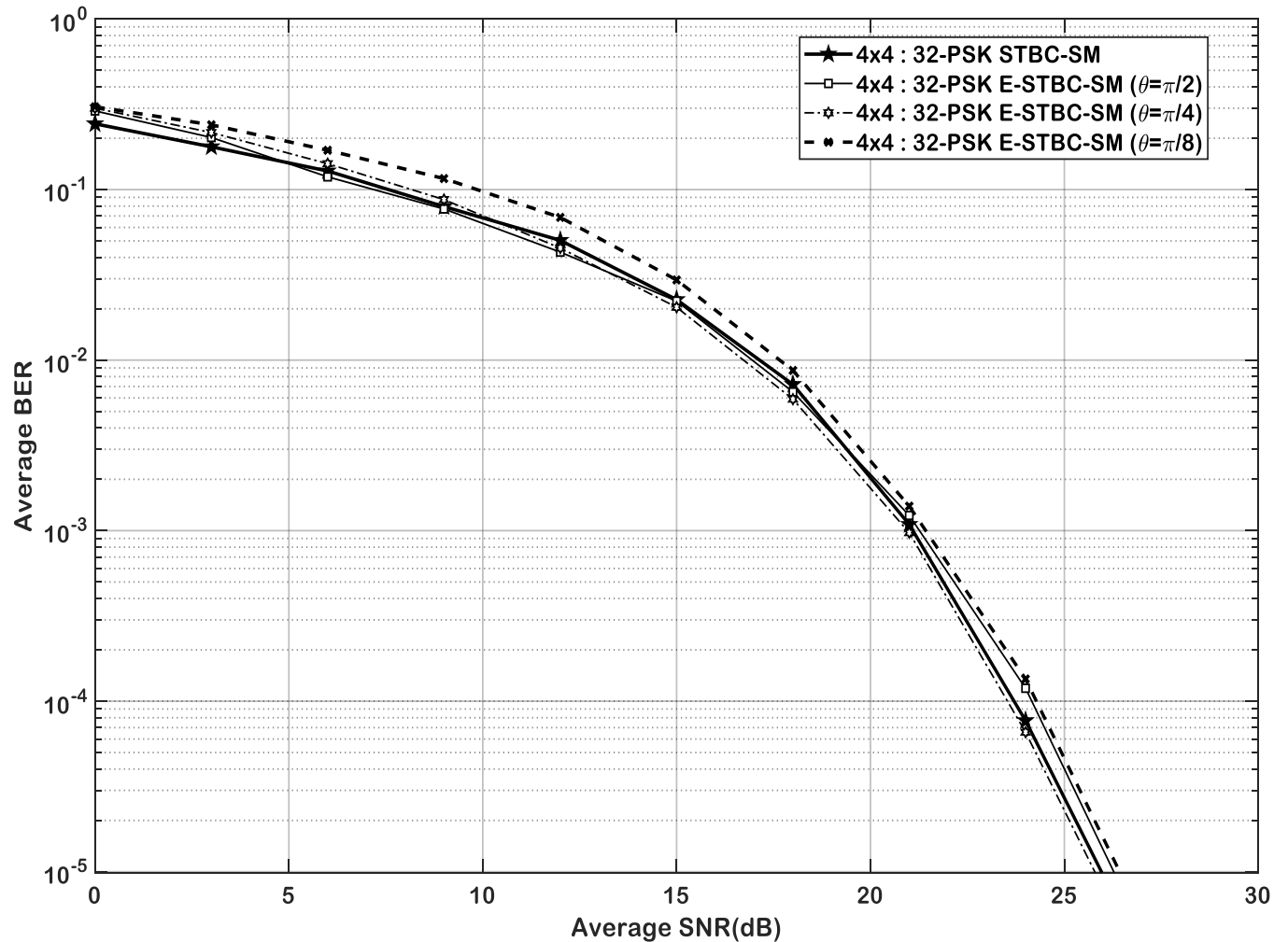


Figure 5-4: BER performance of 32-PSK Alamouti STBC-SM and 32-PSK Alamouti E-STBC-SM

Secondly, Figure 5-4 demonstrate an increase in constellation size i.e. $M = 32$. Both schemes exhibit the same behavior illustrated in Figure 5-3. The diversity of both schemes is similar to the E-STBC-SM scheme having a maximum throughput of 16 bits when $\theta = \frac{\pi}{8}$ as compared to the 12 bits from the conventional STBC-SM scheme. The spectral efficiency of STBC-SM improves by more than 1 b/s/Hz to a maximum of 8 b/s/Hz. This comes at a loss of 0.6 dB in error performance though $\theta = \frac{\pi}{2}$ shows an improvement of 0.2 dB.

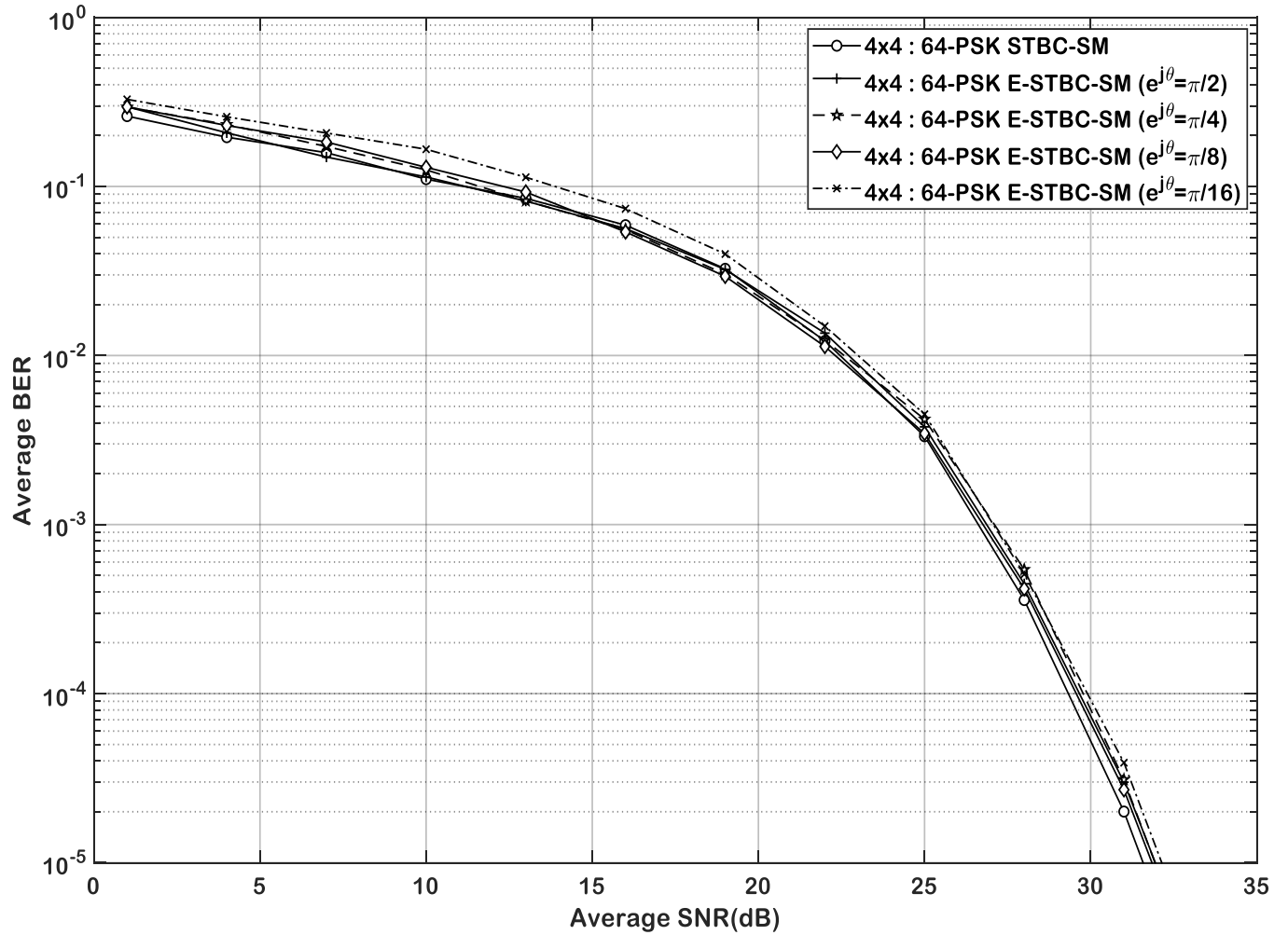


Figure 5-5: BER performance of 64-PSK Alamouti STBC-SM and 64-PSK Alamouti E-STBC-SM

Following the same argument, conventional STBC-SM scheme with $M = 64$ giving a throughput of 14 bits, yields a substantial increase in throughput of 19 bits when rotation angle $\theta = \frac{\pi}{16}$ of the proposed E-STBC-SM scheme. The spectral efficiency improves from 7 b/s/Hz to a maximum of 9.5 b/s/Hz with a maximum attenuation of 0.5 dB in error performance. A summary of results is encapsulated in Table 5-3.

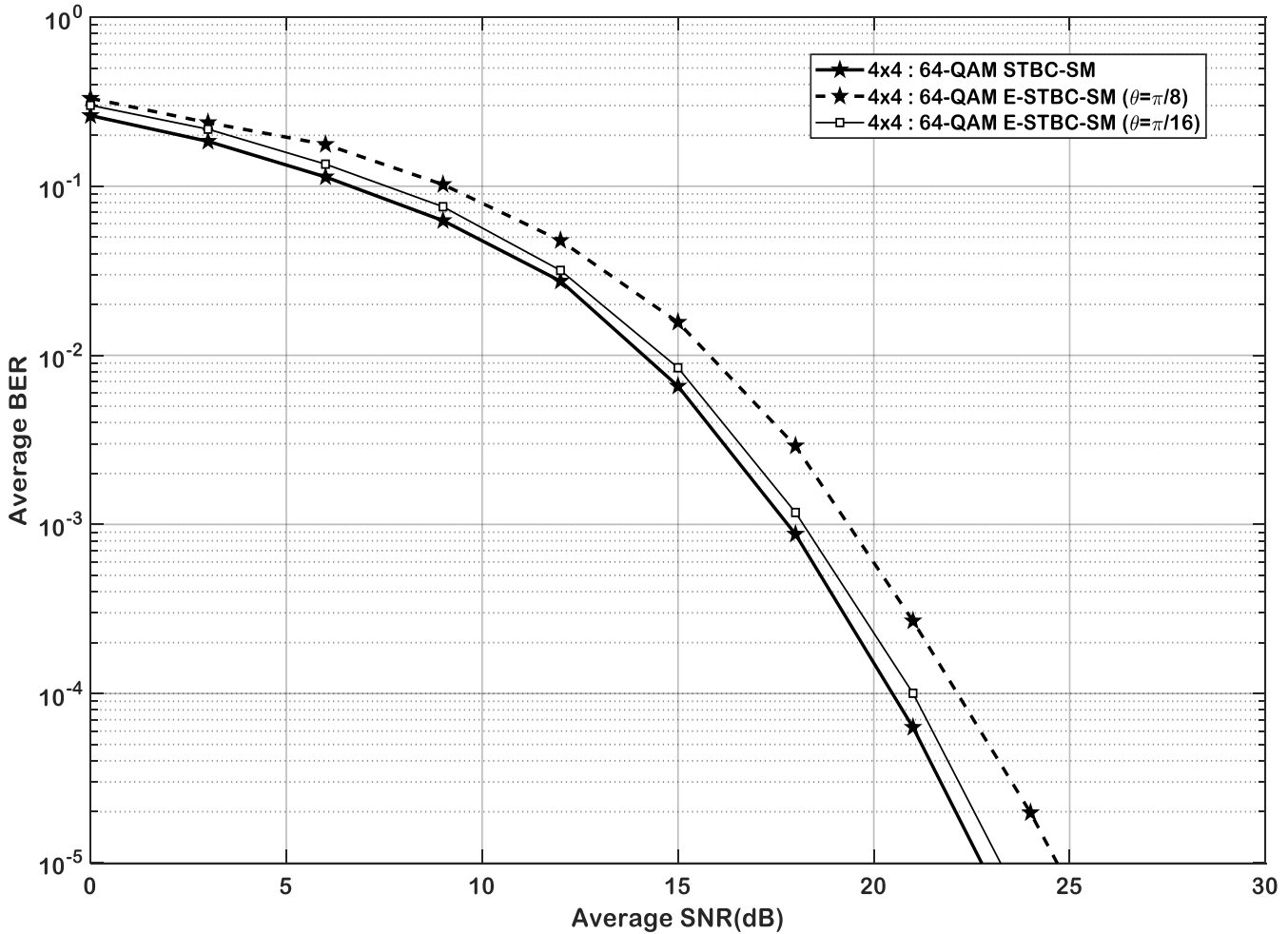


Figure 5-6: BER performance of 64-QAM Alamouti STBC-SM and 64-QAM Alamouti E-STBC-SM

In changing the modulation technique of the STBC symbol pair from PSK to a more spectrum efficient QAM technique, as expected, the error performance improves. Similar to Figure 5-5, the results on Figure 5-6 show an attenuation of 0.5 dB and 2 dB in error performance with rotation angles of $\theta = \frac{\pi}{8}$ and $\frac{\pi}{16}$ though with an overall increase of 4 bits and 5 bits respectively to the conventional STBC-SM scheme. The spectral efficiency also improves from 7 b/s/Hz to 8.5 b/s/Hz and 9.5 b/s/Hz respectively.

Table 5-2: Summary of Throughput, Performance Attenuation, and Spectral Efficiency

Symbols Modulation Order (PSK)	Throughput		Performance Attenuation (dB)	Spectral Efficiency of E- STBC-SM (b/s/Hz)	
	STBC-SM bits	E-STBC-SM			
		θ			Bits
16	10	$\pi/2$	12	0.3	6
		$\pi/4$	13	0.6	6.5
32	12	$\pi/2$	14	-	7
		$\pi/4$	15	0.2	7.5
		$\pi/8$	16	0.4	8
64	14	$\pi/2$	16	0.2	8
		$\pi/4$	17	0.3	8.5
		$\pi/8$	18	0.3	9
		$\pi/16$	19	0.5	9.5

Table 5-2 summarizes comparisons between the proposed E-STBC-SM scheme and conventional STBC-SM scheme. The throughput of both schemes, error performance attenuation between these schemes and spectral efficiency of the E-STBC-SM are depicted.

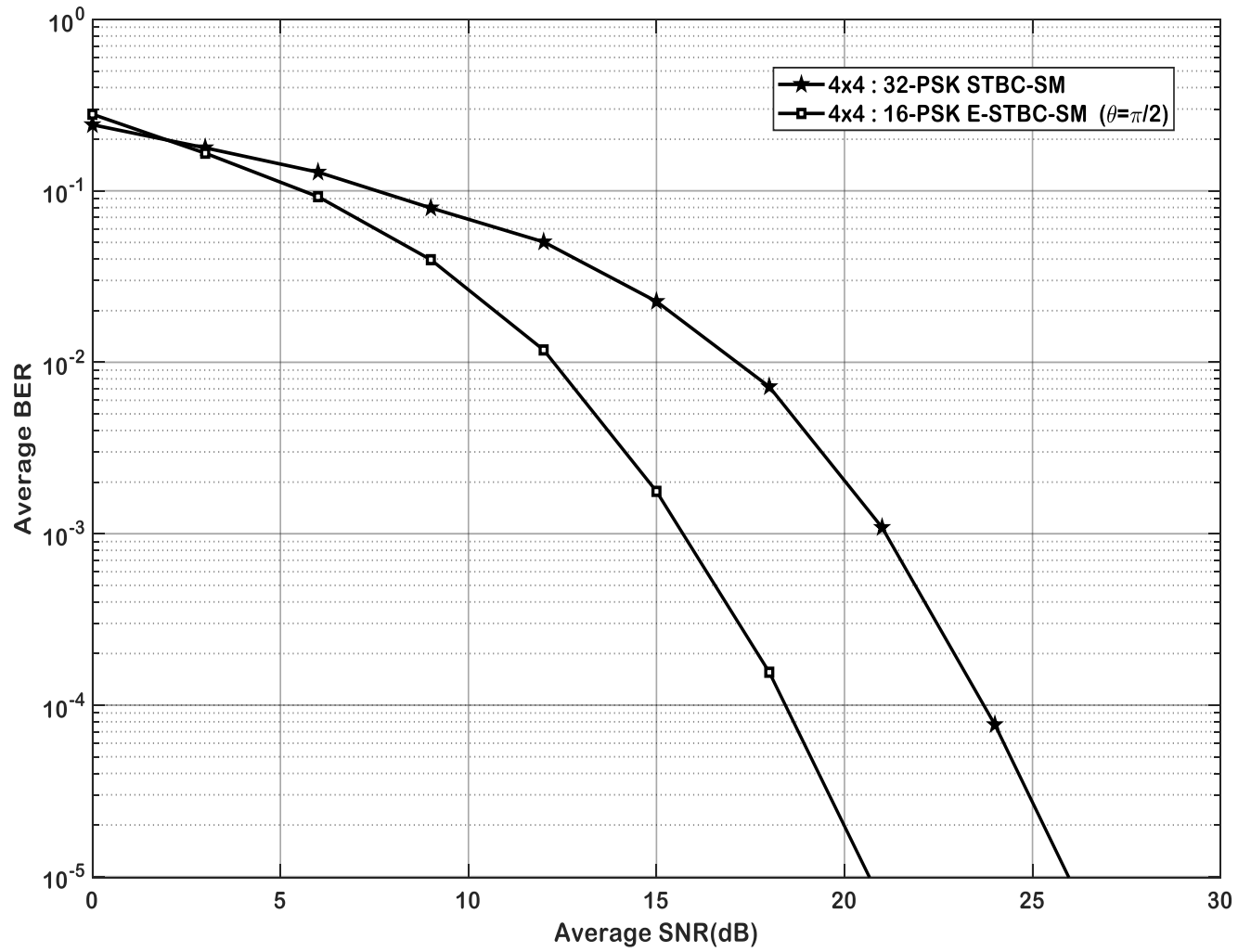


Figure 5-7: Comparing the Performance of systems with 12 bits per frame

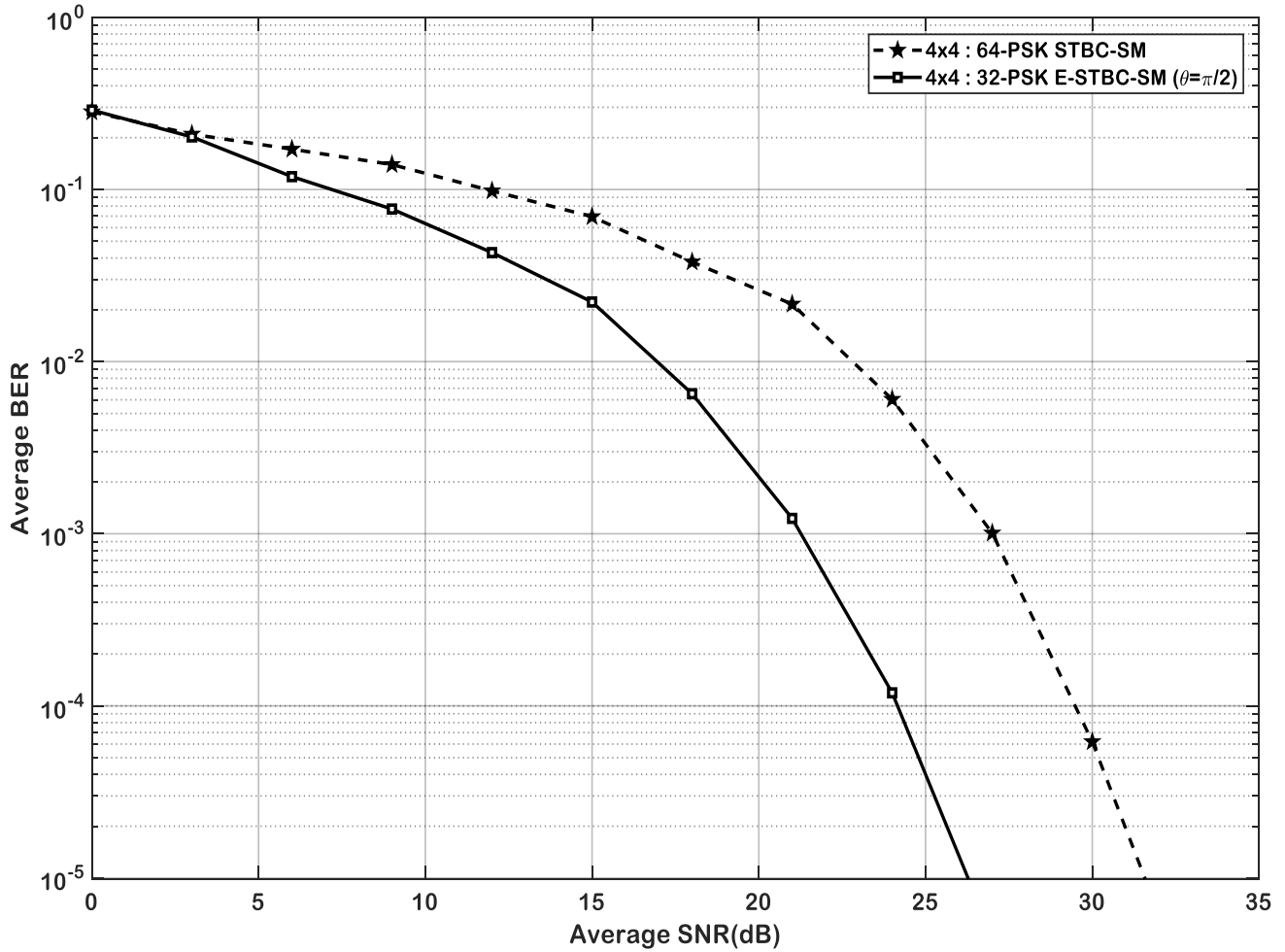


Figure 5-8: Comparing the Performance of systems with 14 bits per frame

Furthermore, Figure 5-7 and Figure 5-8 compare the diversity of the conventional STBC-SM with that of the proposed E-STBC-SM having the same throughput, i.e. systems with 12 and 14 bits per frame. In obtaining the former throughput, we modulate the symbols with PSK where the constellation size $M = 32$ on the conventional STBC-SM scheme where else on the proposed E-STBC-SM scheme the constellation size $M = 16$ with the latter scheme giving a 5-dB diversity gain. For a throughput of 14 bits per frame, the constellation size $M = 64$ for STBC-SM scheme while for E-STBC-SM, $M = 32$. The latter arrangement experiences a 5.4 dB diversity gain. The usage of a smaller modulation size (M) in wireless communication translates to a more reliable system and a better diversity exemplified by the E-STBC-SM scheme.

5.7. Chapter synopsis and conclusion

In this chapter, a spectral efficiency improvement technique for STBC systems was developed. The unitary matrix transformation technique was implemented on the conventional STBC-SM scheme resulting in an enhanced spectral efficiency STBC-SM scheme. This scheme virtually retains the BER performance of the STBC-SM under the same fading channel and additive white Gaussian noise conditions, though a marginal loss in performance is experienced and a slight increase in the computational complexity, higher spectral efficiency is achieved.

Chapter 6

Conclusion and future work

6.1. Conclusion

In this dissertation, a technique that expands the conventional STBC scheme was investigated to further improve the spectral efficiency of the conventional STBC-SM scheme.

An overview of wireless communication systems with the introduction of diversity to transmission schemes through contributions of MIMO system was explored in Chapter 1. Furthermore, in harnessing the power of diversity that achieves coding gain, spectral efficiency, and diversity gain, Alamouti STBC was explored which exploits redundancy to achieve high-performance gain and high reliability in Chapter 2. Monte-Carlo simulations were performed investigating transmit diversity, transmit and receive a diversity of STBC against SISO schemes where the former showed an improvement of over 55% in BER performance. The same diversity gain was achieved by Alamouti STBC against the conventional digital modulation technique with MRC reception while the former suffered from a 3 dB loss in performance.

Limitations of MIMO schemes were remedied in Chapter 3 through the exploration of the SM scheme which eliminates the bottleneck of ICI and IAS experienced in conventional MIMO schemes. Monte-Carlo simulations were performed for different modulation order and antenna configurations over i.i.d. Rayleigh frequency-flat fast fading channels showed to closely match the derived analytical framework at high SNR. Moreover, SM exhibits better BER performance and spectral efficiency when comparing the same number of bpcu against conventional MIMO schemes and MRC.

In Chapter 4 of this dissertation, STBC introduced transmit diversity to SM in a scheme termed STBC-SM which exploits benefits of both STBC and SM. The combining of both MIMO schemes demonstrated a substantial improvement in BER performance matched to the conventional SM scheme. Monte-Carlo simulations over i.i.d. Rayleigh frequency-flat fast fading channels validate the MPSK analytical frame developed which tightly matched. In Table 6-1, a summary of using the same antenna configurations with varying modulation order is detailed.

Table 6-1: SNR gain (dB) of SM compared to STBC-SM at BER of 10^{-5}

Modulation Scheme	SNR gain at BER of 10^{-5} with the 4×4 antenna configuration	
	$M = 8$	$M = 16$
SM	17.47 dB	22.85 dB
STBC-SM	14.24 dB	19.85 dB

Lastly, Chapter 5 in this dissertation details the proposed enhanced spectral efficiency of STBC-SM scheme aimed at improving the spectral efficiency of the conventional STBC-SM scheme. This was achieved by expanding the STBC scheme using unitary matrix transformation thereby improving the throughput. The STBC transmission matrix is multiplied by a diagonal unitary matrix which does not increase the size of the resulting APM symbol set avoiding an increase in the PAPR of the transmitted symbol.

A tight closed-form union bound for MPSK E-STBC-SM over i.i.d. Rayleigh frequency-flat fast fading channels were derived and validated with simulations. Simulation results were presented which showed a substantial improvement in spectral efficiency against the conventional STBC-SM scheme. Evidently, with Monte-Carlo simulation, the E-STBC-SM had a minimal loss peaking at a maximum of 3% in error performance compared to the conventional STBC-SM though a single case with configuration of $M = 32$ and $\theta = \frac{\pi}{4}$ showed a 0.2 dB improvement. Moreover, the improvement was realized at the cost of a slight increase in the computational complexity at the receiver. Table 6-2 summarizes the percentage enhancement in spectral efficiency while Table 6-3 finalizes the percentage error performance attenuation.

Table 6-2: % Spectral Efficiency improvement of E-STBC-SM against STBC-SM

Symbols Modulation Order (PSK)	Spectral Efficiency of the 4×4 antenna configuration			% Spectral Efficiency
	STBC-SM (bpcu)	E-STBC-SM		
		θ	(bpcu)	
16	5	$\pi/2$	6	20
		$\pi/4$	6.5	30
32	6	$\pi/2$	7	16.67
		$\pi/4$	7.5	25
		$\pi/8$	8	33.33
64	7	$\pi/2$	8	14.29
		$\pi/4$	8.5	21.43
		$\pi/8$	9	28.57
		$\pi/16$	9.5	35.71

where the percentage (%) improvement in spectral efficiency of E-STBC-SM in respect to STBC-SM is given as;

$$\% \text{ Spectral efficiency improvement} = \frac{\eta_{E-STBC-SM} - \eta_{STBC-SM}}{\eta_{STBC-SM}} \times 100 \quad (6.1)$$

Table 6-3: % Attenuation of E-STBC-SM against STBC-SM

Symbols Modulation Order (PSK)	SNR gain at 10^{-5} with 4×4 antenna configuration			% Performance Attenuation (-%)
	STBC-SM (dB)	E-STBC-SM		
		θ	(dB)	
16	20.0	$\pi/2$	20.3	1.5
		$\pi/4$	20.6	3
32	26.0	$\pi/2$	25.8	-0.77
		$\pi/4$	26.2	0.77
		$\pi/8$	26.4	1.54
64	31.6	$\pi/2$	31.8	0.63
		$\pi/4$	31.9	0.95
		$\pi/8$	31.9	0.95
		$\pi/16$	32.1	1.58

The percentage performance attenuation is obtained by the difference in BER performance of both schemes given as;

$$\% \text{ performance attenuation} = \frac{\text{BER}_{E\text{-STBC-SM}} - \text{BER}_{\text{STBC-SM}}}{\text{BER}_{\text{STBC-SM}}} \times 100 \quad (6.2)$$

6.2. Future Work

6.2.1 Low complexity detection

The detector of the proposed Enhanced spectral efficiency of STBC-SM (E-STBC-SM) scheme carries out a comprehensive search all over $CN_{\theta}M$ combinations of transmitted symbols, phase symbol and, transmitted antenna pair index. As such, the detector inherits a fairly high computational complexity particularly for high-order symbol and phase constellations which then confines the practicality of this scheme. In accordance to work in [31] and [47], research work could be conducted to remedy the computational complexity overheads which can potentially improve the performance.

6.2.2. Convolutional coding/ TCM

The forward-error-correction is renowned for its ability to control errors in noisy and unreliable channels [47]. Therefore, its use in MIMO systems is appropriate because it can improve the error performance of a system owing to the coding gain [47]. Research work can be conducted in line Govender *et al* [49] to improve the error performance of the proposed E-STBC-SM scheme.

Appendix A

$$P(e^{j\theta_\ell} \rightarrow e^{j\theta_{\hat{\ell}}}|x_1, x_2) = P\left(\begin{array}{l} \|\mathbf{y}_1 - e^{j\theta_\ell} \mathbf{h}_2 x_2\|_F^2 + \|\mathbf{y}_2 + e^{j\theta_\ell} \mathbf{h}_2 x_1^*\|_F^2 \\ > \|\mathbf{y}_1 - e^{j\theta_{\hat{\ell}}} \mathbf{h}_2 x_2\|_F^2 + \|\mathbf{y}_2 + e^{j\theta_{\hat{\ell}}} \mathbf{h}_2 x_1^*\|_F^2 \end{array}\right) \quad (\text{A.1})$$

Substituting (1) into (2) and using the triangular inequality yields;

$$\begin{aligned} P(e^{j\theta_\ell} \rightarrow e^{j\theta_{\hat{\ell}}}|x_1, x_2, \mathbf{h}_2) \\ &= P\left(\|\mathbf{n}_1\|_F^2 + \|\mathbf{n}_2\|_F^2 \right. \\ &> \left. \|\mathbf{h}_2 x_2 (e^{j\theta_\ell} \rightarrow e^{j\theta_{\hat{\ell}}}) + \mathbf{n}_1\|_F^2 + \|\mathbf{h}_2 x_1^* (e^{j\theta_\ell} \rightarrow e^{j\theta_{\hat{\ell}}}) + \mathbf{n}_2\|_F^2\right) \end{aligned} \quad (\text{A.2})$$

The right-hand side of (A.2) simplifies to

$$\|\mathbf{h}_2 x_2 d_1\|_F^2 + \|\mathbf{n}_1\|_F^2 + 2\text{Re}\{\mathbf{n}_1^H \mathbf{h}_2 x_2 d_1\} + \|\mathbf{h}_2 x_1^* d_1\|_F^2 + \|\mathbf{n}_2\|_F^2 + 2\text{Re}\{\mathbf{n}_2^H \mathbf{h}_2 x_1^* d_1\} \quad (\text{A.3})$$

where $d_1 = e^{j\theta_\ell} \rightarrow e^{j\theta_{\hat{\ell}}}$ and subsequently reduces to

$$\begin{aligned} P(e^{j\theta_\ell} \rightarrow e^{j\theta_{\hat{\ell}}}|x_1, x_2, \mathbf{h}_2) \\ &= P(2\text{Re}\{\mathbf{n}_1^H \mathbf{h}_2 x_2 d_1\} + 2\text{Re}\{\mathbf{n}_2^H \mathbf{h}_2 x_1^* d_1\} < -\|\mathbf{h}_2 x_2 d_1\|_F^2 - \|\mathbf{h}_2 x_1^* d_1\|_F^2) \end{aligned} \quad (\text{A.4})$$

Let A_1, A_2 be $\{\mathbf{n}_1^H \mathbf{h}_2 x_2 d_1\}, \{\mathbf{n}_2^H \mathbf{h}_2 x_1^* d_1\}$ and B_1, B_2 be $\|\mathbf{h}_2 x_2 d_1\|_F^2, \|\mathbf{h}_2 x_1^* d_1\|_F^2$ respectively. Hence,

$$\begin{aligned}
P(e^{j\theta_\ell} \rightarrow e^{j\theta_{\hat{\ell}}}|x_1, x_2, \mathbf{h}_2) &= P\left(\text{Re}(A_1 + A_2) < -\frac{1}{2}(B_1 + B_2)\right) \\
&P\left(\text{Re}(A_1 + A_2) > \frac{1}{2}(B_1 + B_2)\right)
\end{aligned} \tag{A.5}$$

Of note,

$\mathbf{n}_1^H \mathbf{h}_2 = n_1^{1*} h_{2,1} + n_1^{2*} h_{2,2} + \dots + n_1^{N_r^*} h_{2,N_r}$, where \mathbf{n}_1^j is a complex Gaussian variable with a distribution $\mathbf{n}_1^j \sim \mathbb{CN}(0, \frac{E_s}{\rho})$. E_s is the average expected energy per symbol and ρ is the signal-to-noise ratio. Therefore, it follows that;

$n_1^{j*} h_{2,j} x_2 d_1$ is a complex Gaussian variable with a distribution $n_1^{j*} h_{2,j} x_2 d_1 \sim \mathbb{CN}\left(0, \frac{E_s \|h_{2,j}\|_F^2 |x_2 d_1|^2}{\rho}\right)$.

Similarly, $\mathbf{n}_1^H \mathbf{h}_2 x_2 d_1 \sim \mathbb{CN}\left(0, \frac{E_s \|\mathbf{h}_2\|_F^2 |x_2 d_1|^2}{\rho}\right)$.

It follows that $\text{Re}\{\mathbf{n}_1^H \mathbf{h}_2 x_2 d_1\} \sim \mathbb{N}\left(0, \frac{E_s \|\mathbf{h}_2\|_F^2 |x_2 d_1|^2}{2\rho}\right)$ and $\text{Re}\{\mathbf{n}_2^H \mathbf{h}_2 x_1^* d_1\} \sim \mathbb{N}\left(0, \frac{E_s \|\mathbf{h}_2\|_F^2 |x_1^* d_1|^2}{2\rho}\right)$ where $\mathbf{n}_1^H \mathbf{h}_2 x_2 d_1$ and $\mathbf{n}_2^H \mathbf{h}_2 x_1^* d_1$ are Gaussian.

Hence, $\text{Re}\{\mathbf{n}_1^H \mathbf{h}_2 x_2 d_1\} + \text{Re}\{\mathbf{n}_2^H \mathbf{h}_2 x_1^* d_1\} \sim \mathbb{N}\left(0, \frac{E_s \|\mathbf{h}_2\|_F^2 |d_1|^2}{2\rho} (|x_1|^2 + |x_2|^2)\right)$.

Therefore,

$$\begin{aligned}
P(e^{j\theta_\ell} \rightarrow e^{j\theta_{\hat{\ell}}}|x_1, x_2, \mathbf{h}_2) &= P\left(\frac{\text{Re}(A_1 + A_2)}{\sqrt{B_3 \frac{E_s}{\rho}}} > \frac{B_3}{\sqrt{B_3 \frac{E_s}{\rho}}}\right) \\
&= P\left(\frac{\text{Re}(A_1 + A_2)}{\sqrt{B_3 \frac{E_s}{\rho}}} > \sqrt{B_3 \frac{\rho}{E_s}}\right)
\end{aligned} \tag{A.6}$$

where $B_3 = \frac{1}{2}(B_1 + B_2)$

$$P\left(\sqrt{B_3 \frac{\rho}{E_s}}\right) = Q\left(\sqrt{B_3 \frac{\rho}{E_s}}\right) \quad (\text{A.7})$$

Hence it follows from (A.6-A.7) that

$$P(e^{j\theta_\ell} \rightarrow e^{j\theta_{\bar{\ell}}}|x_1, x_2, \mathbf{h}_2) = Q\left(\sqrt{\frac{\rho d_2(|x_2|^2 + |x_1^*|^2)\|\mathbf{h}_2\|_F^2}{2E_s}}\right) \quad (\text{A.8})$$

where $d_2 = |d_1|^2$

The general expression received over a Rayleigh fading channel is given as;

$$\mathbf{y} = \sqrt{E_s}\mathbf{h}x + \mathbf{n}$$

where E_s is the energy of the symbol. The instantaneous signal-to-noise ratio of the general Rayleigh fading system is found as follows;

$$\gamma = \frac{E\left\{\|\sqrt{E_s}\mathbf{h}x\|_F^2\right\}}{E\{\|\mathbf{n}\|_F^2\}} = \frac{E_s\mathbf{h}^2}{N_o}$$

where γ is the instantaneous signal-to-noise ratio.

The average signal-to-noise ratio (ρ) is found as follows;

$$\bar{\gamma} = E[\gamma] = \frac{E_s}{N_o} = \rho = \text{average SNR}, \quad E[\|\mathbf{h}\|_F^2] = 1 \text{ and } E[|x|^2] = 1$$

Hence,

$$P(e^{j\theta_\ell} \rightarrow e^{j\theta_{\hat{\gamma}}}|x_1, x_2) = Q(\sqrt{\rho d_2}) \quad (\text{A.9})$$

Now we make use of the Q-function and the trapezoidal rule shown below to manipulate equation (A.9)

The Q-function is given by $Q(x) = \frac{1}{\pi} \int_0^{\frac{\pi}{2}} \exp\left\{-\frac{x^2}{2(\sin w)^2}\right\} dw$ and the Trapezoidal Rule is also given by

$$\int_a^b f(x)dx = \frac{b-a}{n} \left[\frac{f(a) + f(b)}{2} + \sum_{k=1}^{n-1} f\left(a + k\left(\frac{b-a}{n}\right)\right) \right] \quad (\text{A.10})$$

Applying the trapezoidal rule to the Q-function, gives the $Q(x)$ function as;

$$Q(x) = \frac{1}{2n} \left[\frac{e^{-x^2/2}}{2} + \sum_{k=1}^{n-1} \exp\left(\frac{-x^2}{2\sin^2 \frac{k\pi}{2n}}\right) \right] \quad (\text{A.11})$$

where $\theta = \frac{k\pi}{2n}$ and n denote the number of summations for convergence.

Evaluating equation (B.9) into (B.11) yields;

$$Q(\sqrt{\rho d_2}) = \frac{1}{2n} \left[\frac{1}{2} \left(e^{-\frac{\rho d_2}{2}} \right) + \sum_{k=1}^{n-1} e^{-\frac{\rho d_2}{2\sin^2 \theta}} \right] \quad (\text{A.12})$$

Now we introduce the moment generating function (MGF) given by,

$$M(s) = \int_0^\infty e^{-s\gamma} \cdot f_\gamma(\gamma) d\gamma = [1 - s\bar{\gamma}]^{-Nr} \quad (\text{A.13})$$

where $f_\gamma(\gamma) = \frac{1}{\bar{\gamma}} e^{-\left(\frac{\gamma}{\bar{\gamma}}\right)}$ and $\bar{\gamma} = \rho$. Using the MGF on equation (A.12), yields;

$$P(e^{j\theta_\ell} \rightarrow e^{j\theta_{\hat{\gamma}}}) = Q(\sqrt{\rho d_2}) = M(\rho d_2) \quad (\text{A.14})$$

Finally reducing to;

$$P(e^{j\theta_\ell} \rightarrow e^{j\theta_r}) = \frac{1}{2n} \left[\frac{1}{2} \left(\frac{2}{2 + \rho d_2} \right)^{N_r} + \sum_{k=1}^{n-1} \left(\frac{2 \sin^2 \theta}{2 \sin^2 \theta + \rho d_2} \right)^{N_r} \right] \quad (\text{A.15})$$

References

- [1] Q. Ling, and T. Li, “Efficiency improvement for Alamouti codes” *40th Annual Conf. on Info. Science and Systems*, pp. 570-572, March 2006.
- [2] S. Borkar, and H. Pande, “Application of 5G next Generation Network to Internet of Things”, *Int. Con. On the Internet of Things and App. IEEE*, 443-447, Jan. 2016.
- [3] H. Xu, W. Yu, D. Griffith, and N. Golmie, “A Survey on Industrial Internet of Things: A Cyber-Physical System Perspective”, *IEEE Access*, vol. 6, pp 78238-78259, Dec. 2018.
- [4] J. Lin, W. Yu, N. Zhang, X. Yang, H. Zhang, and W. Zhao, “A survey on Internet of Things: Architecture, enabling technologies, security, and privacy, and applications,” *IEEE Internet Things J.*, vol. 4, no. 5, pp. 1125–1142, Oct. 2017.
- [5] R. W. Raut and S. L. Badjate, “Diversity Techniques for Wireless Communication,” *IJARET*, vol. 4, no. 2, pp. 144-160, April 2013.
- [6] E. Basar, U. Aygolu, and E. Panayirci, “Space-time block coded spatial modulation”, *IEEE Trans. On Comm.*, vol. 59, no. 3, pp. 823-832, Mar. 2011.
- [7] M. Kumar, S.P. Sinha, and J. Gupta. “MIMO system for a 5G wireless communication networks: A key to Gigabit wireless system”, *IJISSET*, vol. 2, no. 5, pp. 258-263, May 2015.
- [8] S. K. Sharma and S. N. Ahmad, “Performance of MIMO Space-Time Coded Wireless Communication System,” *IEEE ICCIMA*, vol. 4, pp. 373—377, 2007.
- [9] N. Parveen, D.S. Venkateswarlu, “Implementation of Space-Time Block coding using 2 Transmit and 2 Receive Antennas”, *IJETAE*, vol. 2, no. 10, pp.175-178, Oct. 2012.
- [10] V. Kühn, “Multiple Antenna Systems,” in *Wireless Communications Over MIMO Channels*. John Wiley & Sons Ltd, pp. 282-289, 2006.
- [11] R. Mesleh, H. Haas, C. W. Ahn, and S. Yun, “Spatial Modulation - A New Low Complexity Spectral Efficiency Enhancing Technique,” in *Proc. ChinaCOM, Beijing*, pp. 1-5, Oct. 2006.
- [12] H. Lee, M. Siti, W. Zhu, and M. Fitz, “Super-orthogonal space-time block code using a unitary expansion,” in *IEEE 60th Annual Conference on Vehicular Technology*, Los Angeles, Sep. 2004.
- [13] J. G. Proakis, “Multichannel and Multicarrier systems”, *Digital Communications*, 4th ed., New York, McGraw-Hill, ch. 12, pp. 680-681, 2001.

- [14] K. M. Noga and B. Palczynska, "Overview of fading channel modeling," *International journal of electronics and telecommunications*, vol. 56, no. 4, pp.339-344, 2010.
- [15] B. Vucetic and J. Yuan, "Space-Time Coding Performance Analysis and Code Design," *Space-time Coding*, John Wiley & Sons, ch. 2, pp. 54–58, 2003.
- [16] J. Boutros and E. Viterbo, "Signal Space Diversity: A Power- and Bandwidth-Efficient Diversity Technique for the Rayleigh Fading Channel," *IEEE Transactions on Information Theory*, vol. 44, no. 4, pp. 1453-1467, July 1998.
- [17] W. T. Chen, "Spectral efficiency analysis for LTE networks," *IEEE*, pp. 93-95, 2014.
- [18] S. Alamouti, "Simple transmit diversity technique for wireless communications", *IEEE J. Select. Area Communications*, vol. 16, no.8, pp. 1451-1458, Oct. 1998.
- [19] V. Tarokh, N. Seshadri, and A. R. Calderbank, "Space-Time Codes for High Data Rate Wireless Communication: Performance Criteria and Code Construction," *IEEE Transactions on Information Theory*, vol. 44, no. 2, pp. 744-765, Mar.1998.
- [20] V. Tarokh, H. Jafarkhani, and A. R. Calderbank, "Space-time block codes from orthogonal designs," *IEEE Trans. Inf. Theory*, vol. 45, no. 5, pp. 1456-1467, Jul. 1999.
- [21] G. J. Foschini, M. J. Gans, and J. M. Khan, "Fading Correlation and its Effect on the Capacity of Multi-Element Antenna System," *IEEE Transactions on Communications*, vol.48, no. 3, pp 502-513, Mar. 2000.
- [22] S. Loyka and G. Tsoulos, "Estimating MIMO System Performance Using the Correlation Matrix Approach," *IEEE Comm. Letters*, vol.6, no. 1, pp. 19-21, Jan. 2002.
- [23] M. Chiani, M. Z. Win, and A. Zanella, "On the Capacity of Spatially Correlated MIMO Rayleigh-Fading Channels," *IEEE Transactions on Information Theory*, vol.49, no.10, pp. 2363-2371, Oct. 2003.
- [24] S. Catreux, P. F. Driessen, and L. J. Greenstein, "Simulation Results for an Interference-Limited Multiple-Input Multiple-Output Cellular System," *IEEE Communication Letters*, vol. 4, no. 11, pp. 334-336, Nov. 2000.
- [25] G. J. Foschini, "Layered Space-Time Architecture for Wireless Communication in a Fading Environment when using Multi-Element Antennas," *Bell Labs Technical Journal*, vol. 1, no. 2, pp. 41-59, Sep. 1996.

- [26] V. Tarokh, A. Naguib, N. Seshadri, and A. R. Calderbank, "Space-time codes for wireless communication: Combined away processing and space-time coding," *IEEE Transactions on Information Theory*, Mar. 1998.
- [27] S. Saranya Pauline and C. Veeralakshmi, "A Survey on Various Receivers for UWB Communication," *IOSR Journal of Electronics and Communication Engineering*, vol. 7, no. 6, pp. 7-11, Oct. 2013.
- [28] R. Mesleh, H. Haas, S. Sinanovic, C.W. Ahn, and S. Yun, "Spatial Modulation," *IEEE Transactions on Vehicular Technology*, vol. 57, no. 4, pp. 2228-2241, July 2008.
- [29] R. Mesleh, H. Haas, A. Ghrayeb, S. Yun and L. Hanzo, "Spatial Modulation for Generalized MIMO: Challenges, Opportunities and Implementation," *IEEE Proceedings*, vol. 102, no. 1, pp. 55-103, Jan. 2014.
- [30] R. Mesleh, H. Haas, C.W. Ahn, and S. Yun, "Spatial Modulation – A new low complexity spectral efficiency enhanced technique," *IEEE First International Conference on Communications and Networking in China*, Oct. 2006.
- [31] H. Xu and N. Pillay, "Simple near-maximum-likelihood low-complexity detection scheme for Alamouti space-time block coded spatial modulation," *IET Communications*, vol. 8, no. 5, pp. 2611-2618, May 2014.
- [32] H. Xu, K. Govindasamy, and N. Pillay, "Uncoded space-time labeling diversity," *IEEE Communications Letters*, vol.20, no. 8, pp. 1511-1514, August 2016.
- [33] D. Varshney, C. Arumugam, V. Vijayaraghavan, N. Vijay, S. Srikanth, "Space-time codes in wireless communications", *IEEE Potentials*, vol. 22, no. 3, pp. 36-38, Sept. 2003.
- [34] V. Tarokh, H. Jafarkhani, and A. R. Calderbank, "Space – Time Block Codes from Orthogonal Designs," *IEEE Transactions on Information Theory*, vol. 45, no. 5, pp. 1456–1467, 1999.
- [35] R. M. Legnain, R. H. M. Hafez, I. D. Marsland, and A. M. Legnain, "A Novel Spatial Modulation Using MIMO Spatial Multiplexing", *ICCSPA*, vol. 1, 12-14 Feb. 2013.
- [36] J. Jeganathan, A. Ghrayeb, and L. Szczecinski, "Spatial Modulation: Optimal Detection and Performance Analysis," *IEEE Communications Letter*, vol. 12, no. 8, pp. 545-547, Aug. 2008.
- [37] R. Mesleh, M. Di Renzo, P.M. Grant, "Trellis-Coded Spatial Modulation", *IEEE Transactions on Communications*, vol. 9, no. 7, pp.2349-2361, July 2010.
- [38] N. R. Naidoo, H. Xu and T. Quazi, "Spatial Modulation: Optimal Detector Asymptotic Performance and Multiple-stage Detection," *IET Communications*, vol. 5, no. 10, pp. 1368-1376, Jul. 2011.

- [39] M. K. Simon, and M.S. Alouini, "A Compact Performance Analysis of Generalized Selection Combining with Independent but Nonidentically Distributed Rayleigh Fading Paths", *IEEE Transactions on Communications*, vol. 50, no. 9, Sept. 2002
- [40] J. Jeganathan, A. Ghrayeb, L. Szczecinski, and A. Ceron, "Space shift keying modulation for MIMO channels," *IEEE Transactions on Wireless Communications.*, vol. 8, no. 7, pp. 3692-3703, July 2009.
- [41] M.T. Le, V.D. Ngo, H.A. Mai, and X.N. Tran, "High-rate Space-Time Block Coded Spatial Modulation," *International conference on Advances Technologies for Communications*, pp. 278-282, 2012.
- [42] X. Li and L. Wang, "High rate Space-Time Block coded Spatial Modulation with Cyclic Structure," *IEEE Communications Letters*, vol. 18, no.4, pp 532-535, April 2014.
- [43] Binh T Vo, Ha H Nguyen, and Nguyen Quoc-Tuan. "High-rate space-time block coded spatial modulation". *Advanced Technologies for Communications (ATC)*, 2015 International Conference on. IEEE, pp. 1–5, 2015.
- [44] Heechoon Lee et al. "Super-orthogonal space-time block code using a unitary expansion". *Vehicular Technology Conference*, 2004. VTC2004-Fall. 2004 IEEE 60th. Vol. 4. IEEE, pp. 2513–2517, 2004.
- [45] S. S. H. Bidaki, S. Talebi, and M. Shahabinejad, "A full-rate full-diversity 2×2 space-time block code with linear complexity for the maximum likelihood receiver," *IEEE Communications Letters*, vol. 15, no. 8, pp. 842-844, Aug. 2011.
- [46] L. Xiao, P. Xiao, Y. Xiao, C.Wu, H.V. Nguyen, I. Hemadeh and L. Hanzo, "Transmit Antenna Combination Optimization for Generalized Spatial Modulation systems" *IEEE Access*, vol.6, pp.41866-41882, July 2018.
- [47] I. Al-Shahrani, "Performance of M-QAM over generalized mobile fading channels using MRC diversity," M.S thesis King Saud University, Riya, Saudi Arabia, Feb. 2007.
- [48] R. Govender, N. Pillay, and H. Xu," Soft-output space-time block coded spatial modulation," *IET Communications*, vol. 8, no. 16, pp. 2789-2798, Feb. 2014.
- [49] A. Goldsmith. "Performance of digital modulation over wireless channels," in *Wireless Communications*. Cambridge University Press, pp. 159-177, 2005.
- [50] Moon, T.K.: 'Error correction coding: mathematical methods and algorithms' (Wiley, 2005)